Automated Code Generation for Many-Body Perturbation Theory Diagrams

Christian Drischler (drischler@ohio.edu)

Automated tools for many-body theory

June 7, 2023 | Espace de Structure Nucléaire Théorique (CEA/DSM-DAM)

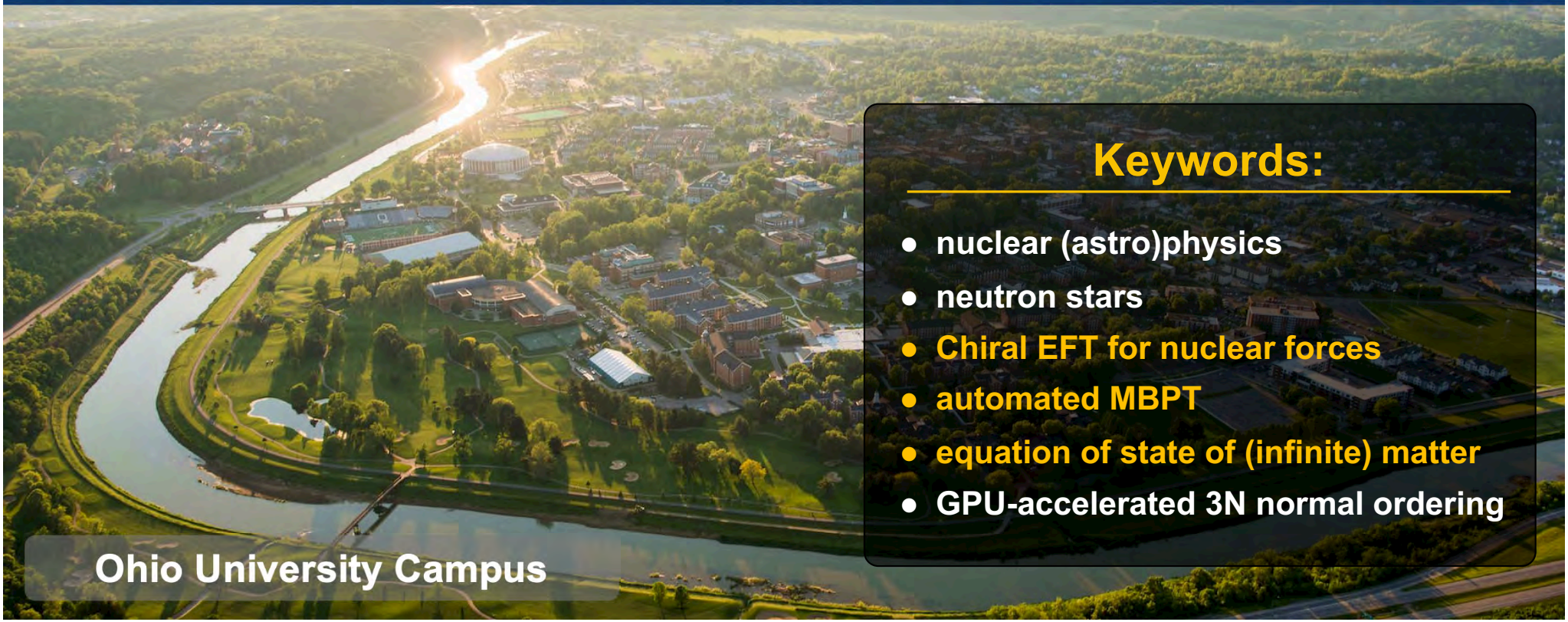

Keywords:

- nuclear (astro)physics
- neutron stars
- Chiral EFT for nuclear forces
- automated MBPT
- equation of state of (infinite) matter
- GPU-accelerated 3N normal ordering

Neutron stars…

OHIO UNIVERSITY

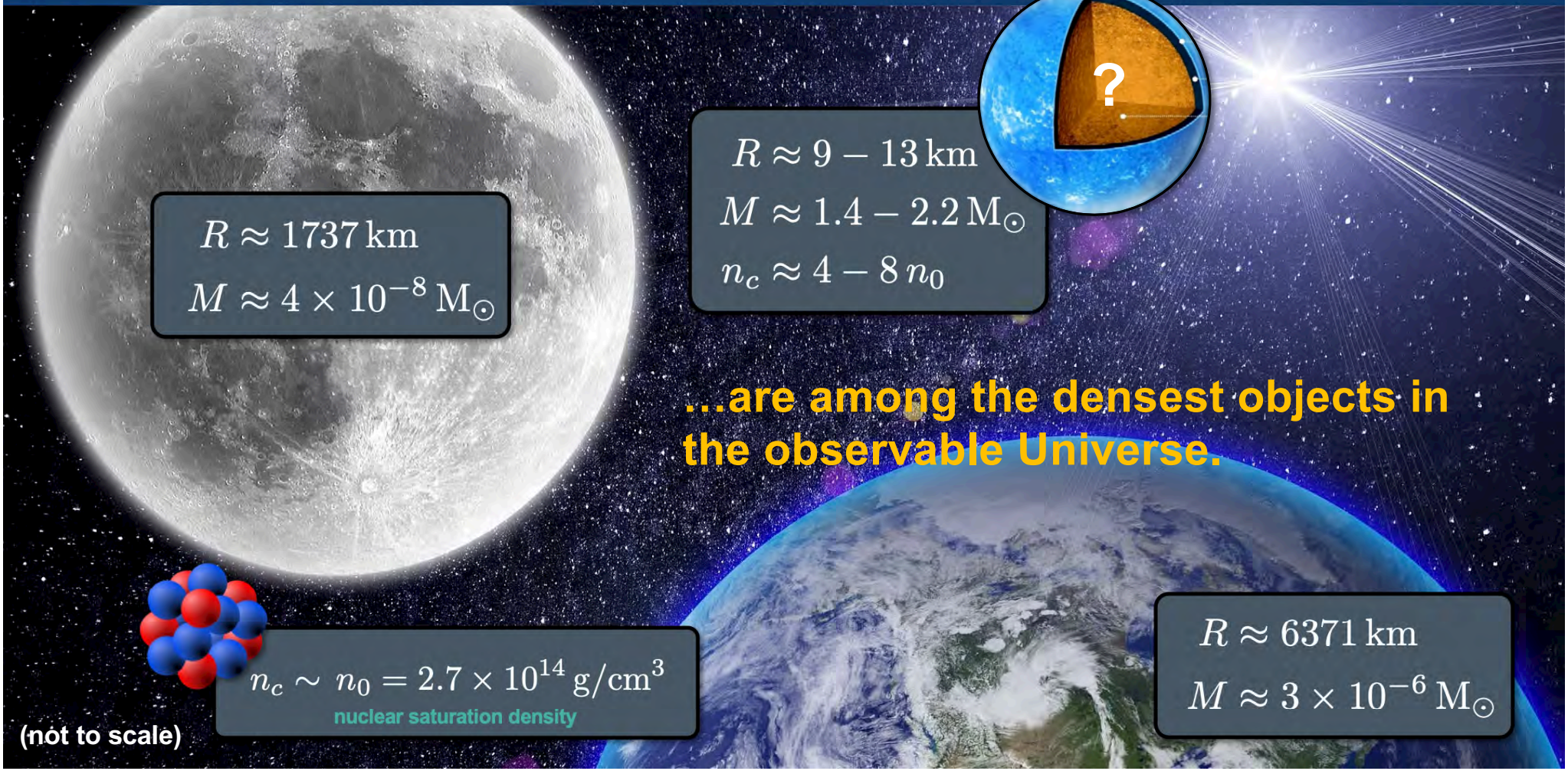

GW170817: first binary neutron star merger observed

OHIO UNIVERSITY

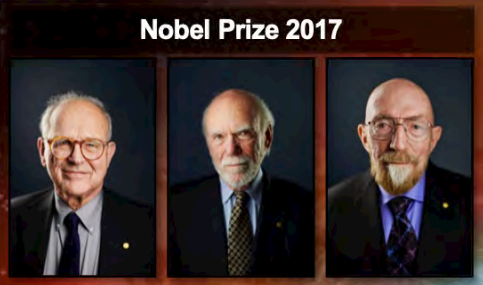

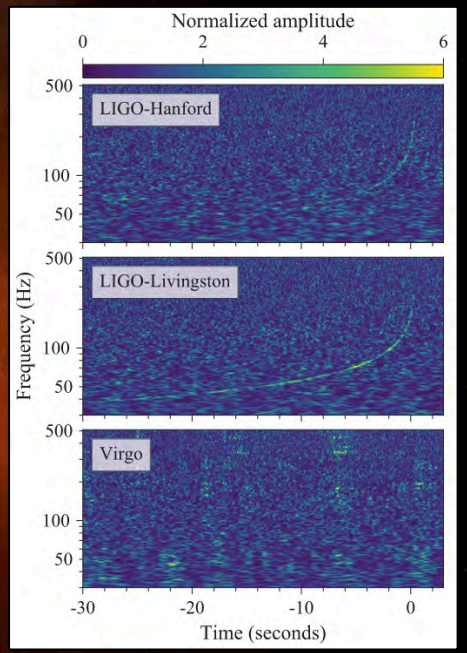

Multi-messenger event:

- gravitational waves
- electromagnetic signals
  - GRB170817A
  - AT2017gfo

Multi-Messenger Astronomy has opened a new window to the Universe

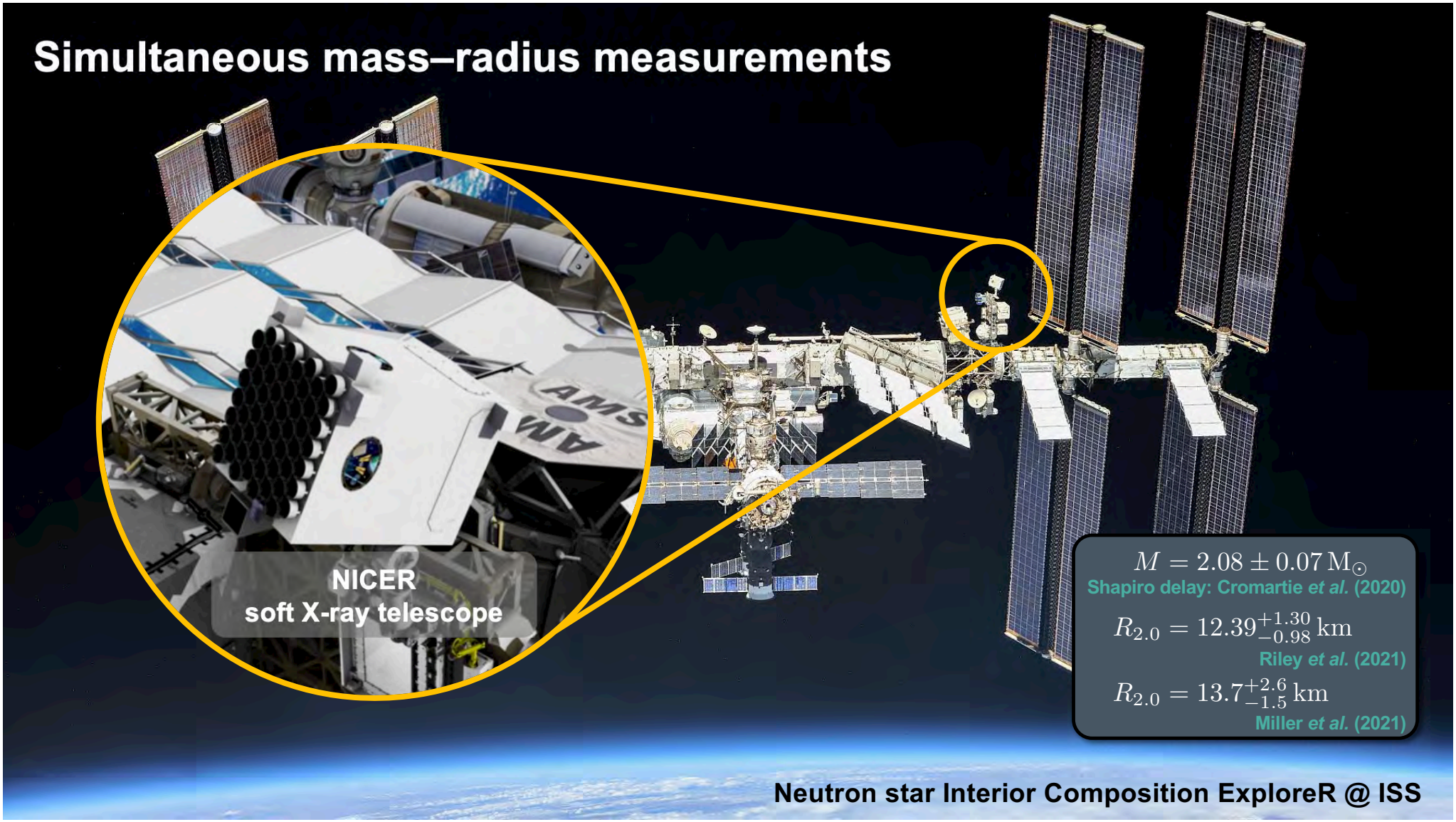
Simultaneous mass–radius measurements
NICER
soft X-ray telescope
$M = 2.08 \pm 0.07\,\mathrm{M}_\odot$
Shapiro delay: Cromartie et al. (2020)
$R_{2.0} = 12.39^{+1.30}_{-0.98}\,\mathrm{km}$
Riley et al. (2021)
$R_{2.0} = 13.7^{+2.6}_{-1.5}\,\mathrm{km}$
Miller et al. (2021)
Neutron star Interior Composition ExploreR @ ISS

Structure of cold neutron stars

OHIO UNIVERSITY

hydrostatic equilibrium

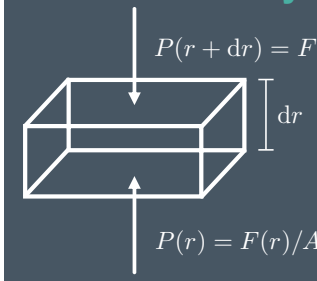

+ General Relativity

Tolman–Oppenheimer–Volkoff equation

$$\frac{dP}{dr} = -\frac{(\varepsilon + P)(m + 4\pi r^3 P)}{r(r - 2m)} \qquad \frac{dm}{dr} = 4\pi r^2 \varepsilon$$

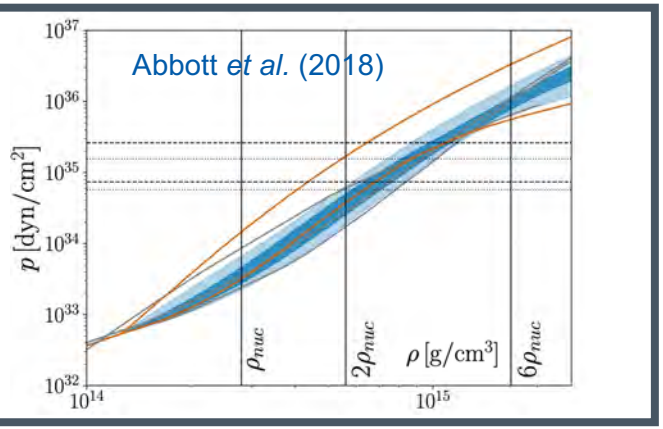

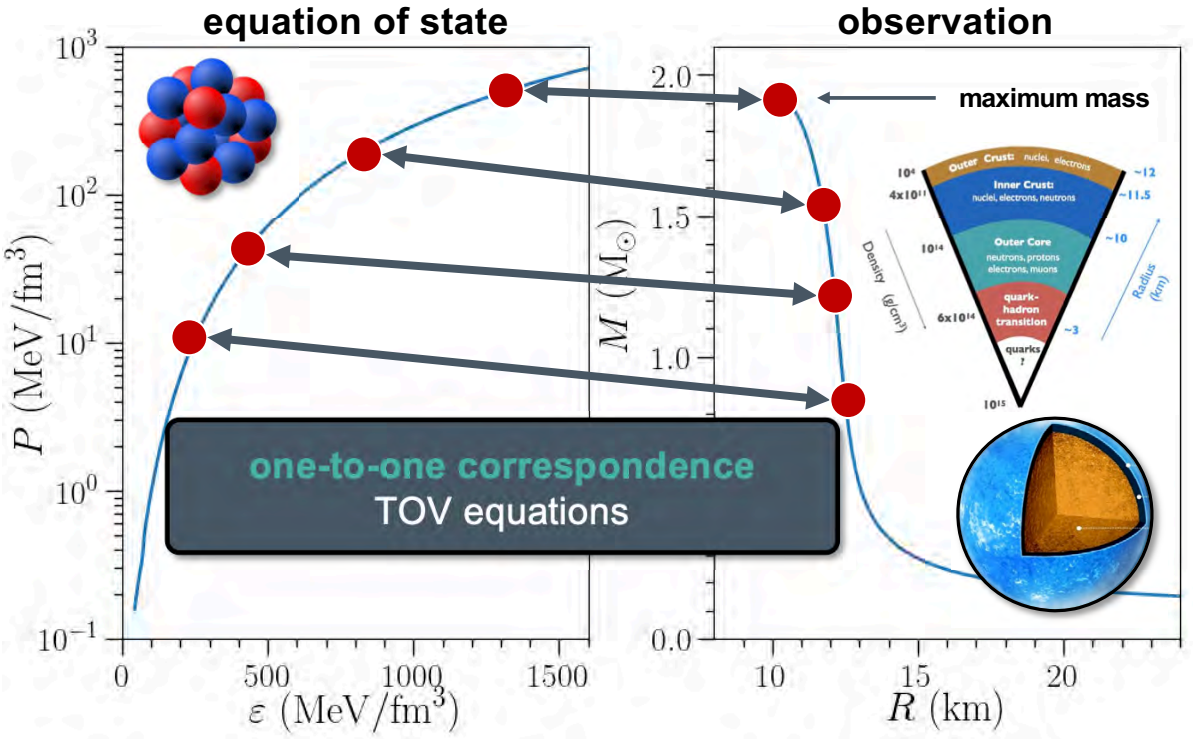

Credit: A. Steiner

The general relativistic equation for hydrostatic equilibrium determines the neutron star structure

FRIB and FRIB Science

Facility for Rare Isotope Beams
at Michigan State University

OHIO UNIVERSITY

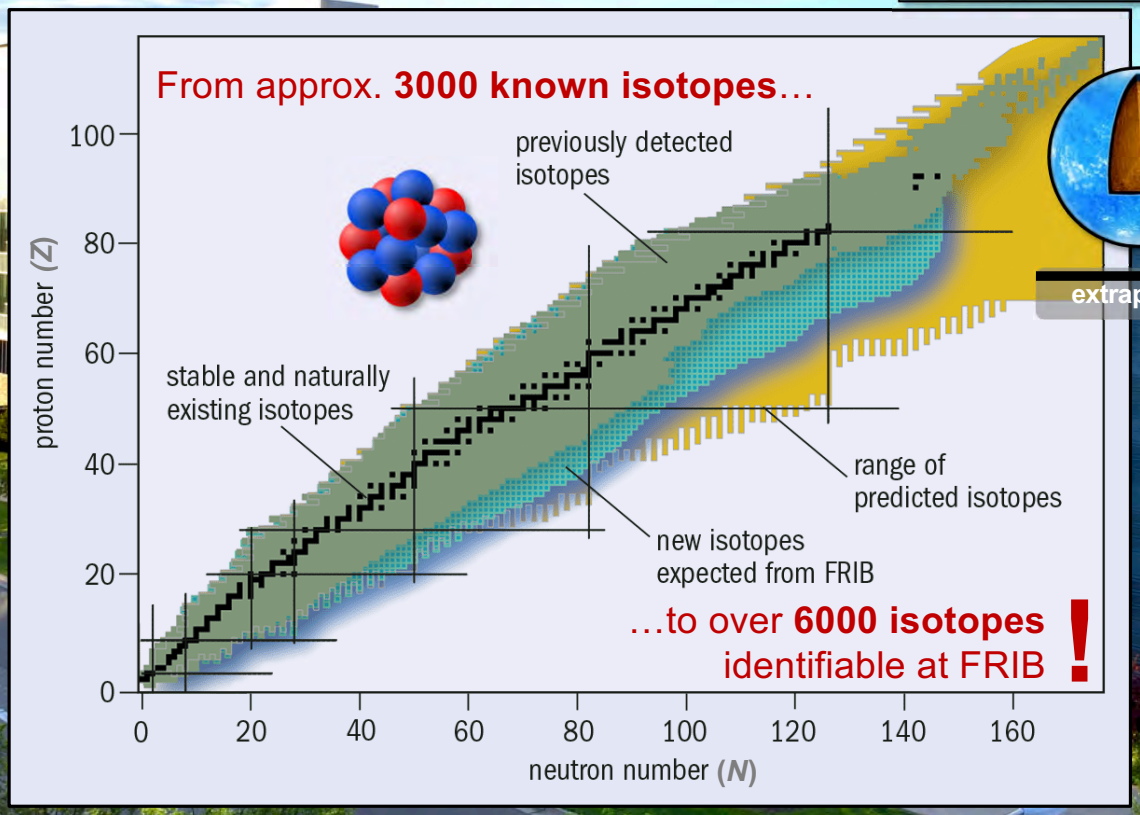

extrapolate

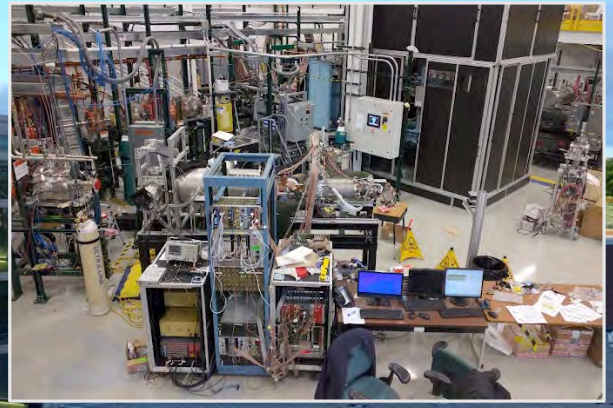

New rare isotope research facility

+ other beam facilities world-wide: FAIR, SPIRAL2…

Opportunity & challenge for nuclear theory

OHIO UNIVERSITY

Coordinated efforts are paramount:

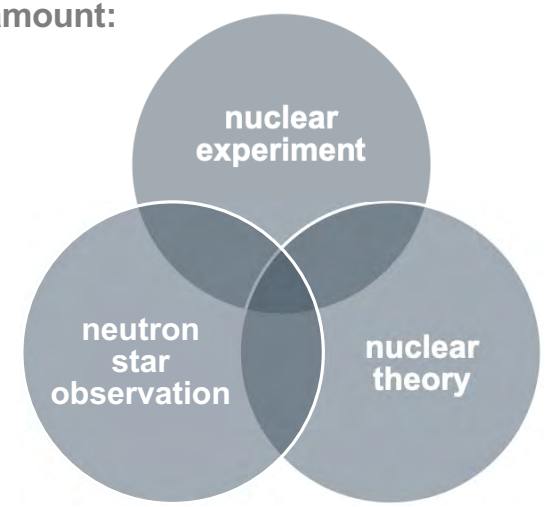

We just entered a **Golden Era for Nuclear Physics & Astrophysics**

unique opportunity to obtain a **fundamental understanding** of strongly interacting matter, with great **potential for discovery**

Nuclear theory: How do we

- **interpret** these experiments & observations *microscopically*
- **predict** outcomes when experiments are *not* feasible
- **quantify & propagate** our **theoretical uncertainties**

Overarching questions include:

- How do **nuclear phenomena** emerge from fundamental principles?
- Where do **heavy elements** like Gold come from?
- How are **stars** born? And how do they die?

Major efforts:

Bayesian methods for calibration, uncertainty quantification and propagation, experimental design, sensitivity studies, …

Reduced Order Models (ROM) enable these methods, especially efficient MC sampling of model parameter spaces

Last week's ESNT workshop *Eigenvector continuation method in nuclear structure and reaction theory* (slides available): https://esnt.cea.fr/Phocea/Page/index.php?id=109

Ab initio workflow (idealized)

OHIO UNIVERSITY

uncertainty quantification
(truncation errors, many-body approximations, ...)

nuclear observables
(structure, reactions, astrophysics, ...)

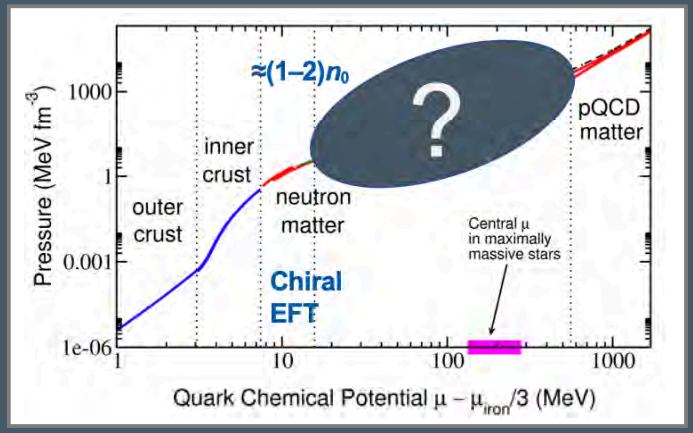

quantum chromodynamics
(CalLat, HALQCD, NPLQCD, ...)

CD & Bogner, Few Body Syst. **62**, 109

Here: nuclear equation of state (EOS)

energy per particle (and derived quantities)

$$\frac{E}{A}(n, \delta, T)$$

baryon density n
neutron excess δ
temperature T

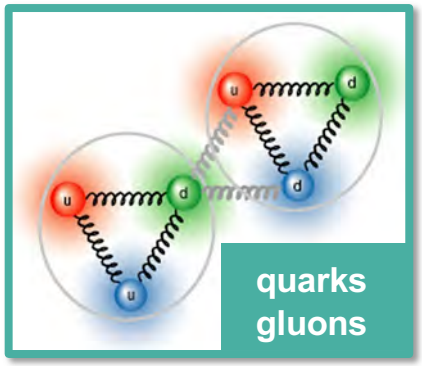

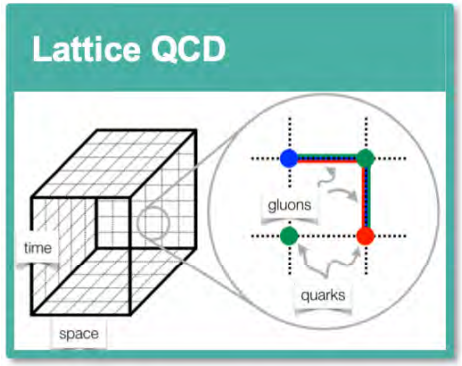

theory of strong interactions

QCD is nonperturbative at the low energies relevant for nuclear physics (cf. pQCD & LQCD)

CD, Haxton, McElvain, Mereghetti *et al.*, PPNP **121**, 103888

Ab initio workflow (idealized)

OHIO UNIVERSITY

$$H(\boldsymbol{\theta})\,|\psi(\boldsymbol{\theta})\rangle = E(\boldsymbol{\theta})\,|\psi(\boldsymbol{\theta})\rangle$$

Schrödinger Equation

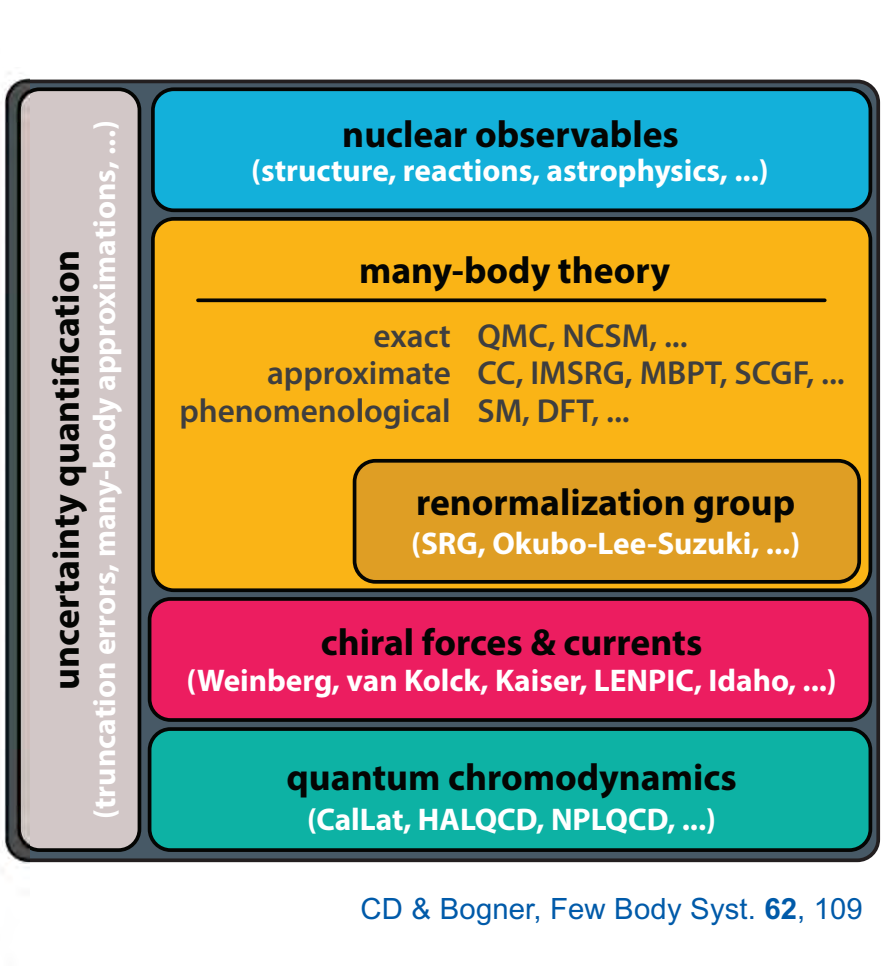

CD & Bogner, Few Body Syst. **62**, 109

Here: nuclear equation of state (EOS)
energy per particle (and derived quantities)

$$\frac{E}{A}(n,\delta,T)$$

baryon density n
neutron excess δ
temperature T

computational framework
solves the (many-body) Schrödinger equation
requires a nuclear potential as input

chiral effective field theory
provides microscopic interactions consistent with the symmetries of *low-energy* QCD

theory of strong interactions
QCD is nonperturbative at the low energies relevant for nuclear physics (cf. pQCD & LQCD)

Major process: CEFT, many-body theory, and UQ!

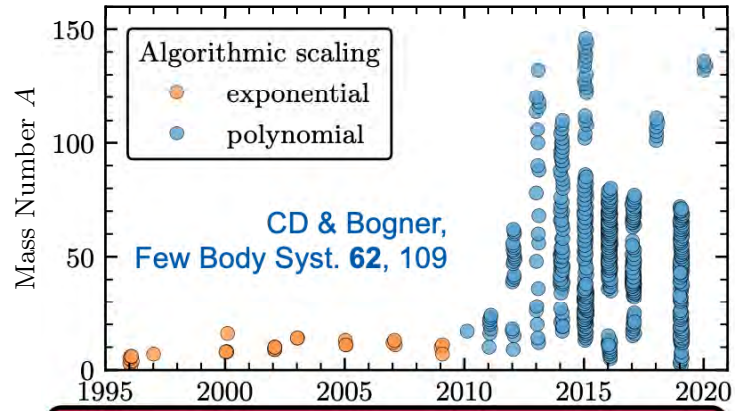

nuclear physics in the precision era
limitations due to NN+3N forces

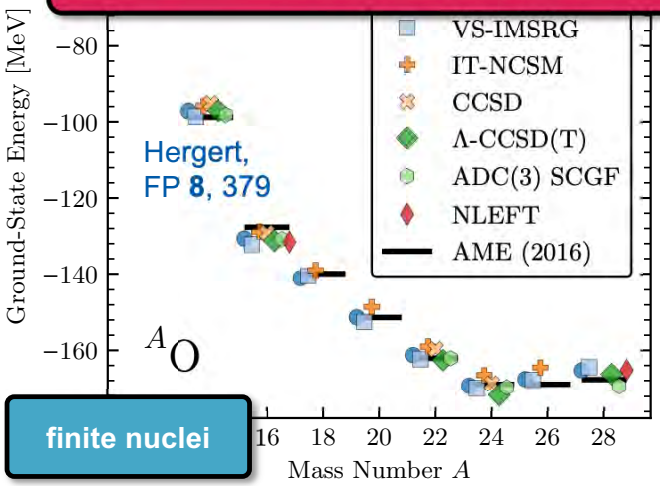

finite nuclei

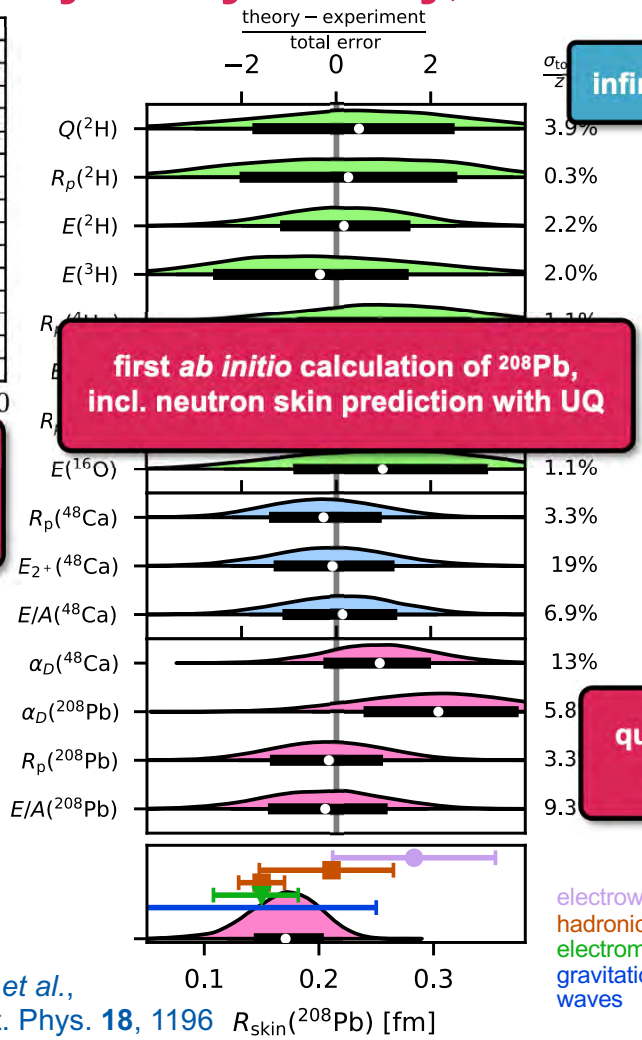

Hu *et al.*,
Nat. Phys. **18**, 1196

first *ab initio* calculation of ^{208}Pb,
incl. neutron skin prediction with UQ

infinite matter

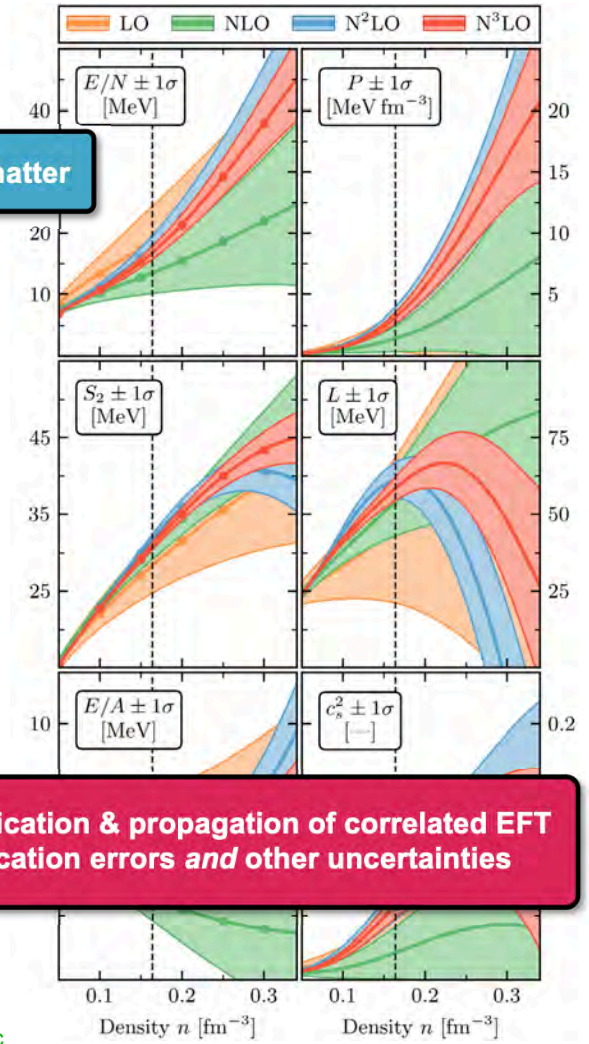

quantification & propagation of correlated EFT
truncation errors *and* other uncertainties

CD, Furnstahl, Melendez,
Phillips, PRL **125**, 202702

electroweak
hadronic
electromagnetic
gravitational
waves

Ab initio workflow (idealized)

OHIO UNIVERSITY

$$H(\boldsymbol{\theta})\,|\psi(\boldsymbol{\theta})\rangle = E(\boldsymbol{\theta})\,|\psi(\boldsymbol{\theta})\rangle$$

Schrödinger Equation

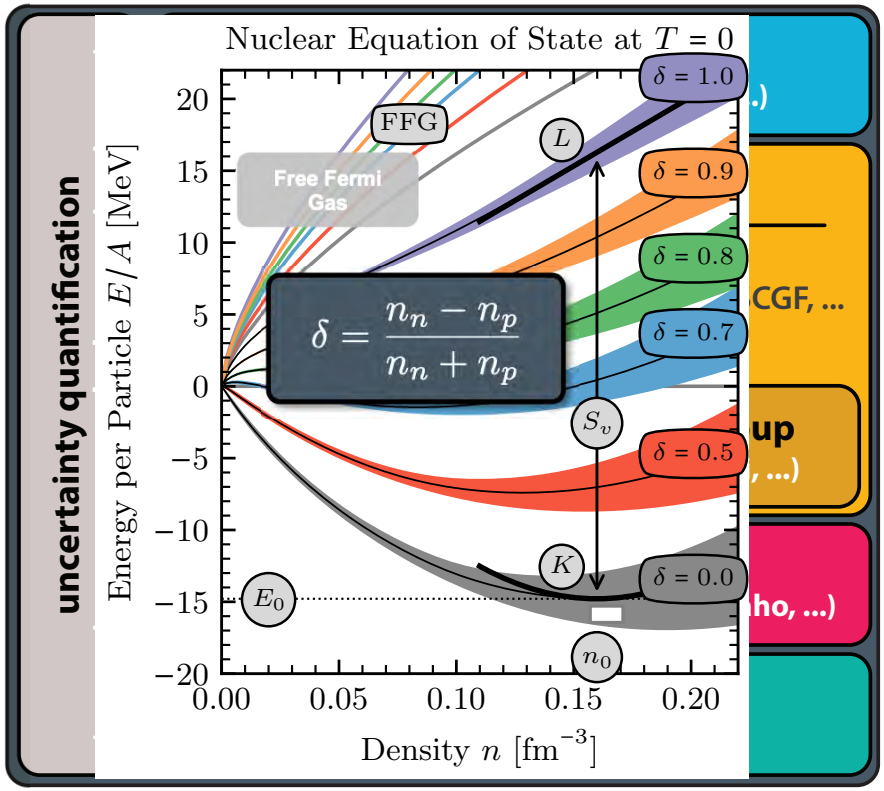

CD & Bogner, Few Body Syst. **62**, 109

Here: nuclear equation of state (EOS)
energy per particle (and derived quantities)

$$\frac{E}{A}(n, \delta, T)$$

baryon density n
neutron excess δ
temperature T

Here: many-body perturbation theory (MBPT)

computationally efficient method (HPC-friendly)
allows to estimate many-body uncertainties

Widely applicable:

- ✓ arbitrary proton fractions
- ✓ finite temperature
- ✓ optical potentials, linear response, nuclei, …

Other frameworks include **quantum Monte Carlo**, coupled cluster, and self-consistent Green's functions

Many-body perturbation theory (MBPT) in a nutshell

OHIO UNIVERSITY

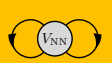

$$\frac{E^{(0)}}{V} = +\frac{1}{2}\sum_{ij}\langle ij\,|\,\overline{V}_{\rm NN}\,|\,ij\rangle$$

Hartree-Fock

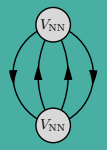

$$\frac{E^{(2)}}{V} = \frac{1}{4}\sum_{\substack{ij\\ab}}\frac{|\langle ij|\overline{V}_{\rm NN}|ab\rangle|^2}{\varepsilon_i+\varepsilon_j-\varepsilon_a-\varepsilon_b}$$

second order

$$|i\rangle = |\mathbf{k}_i\sigma_i\tau_i\rangle$$

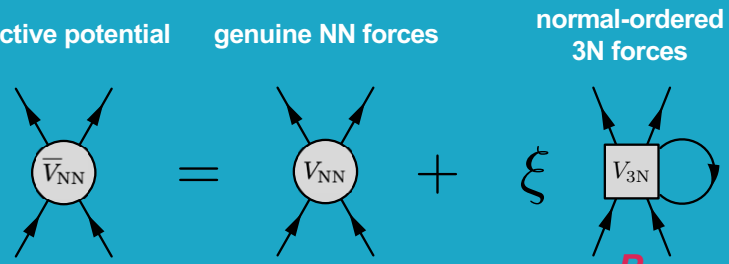

typically requires approximations | involved at N³LO+

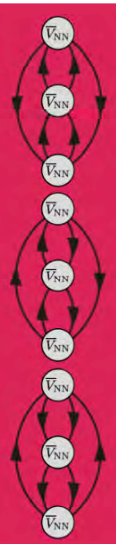

$$\frac{E^{(3)}_{hh}}{V} = +\frac{1}{8}\sum_{\substack{ab\\ijkl}}\frac{\langle ij\,|\,\overline{V}_{\rm NN}\,|\,ab\rangle\langle kl\,|\,\overline{V}_{\rm NN}\,|\,ij\rangle\langle ab\,|\,\overline{V}_{\rm NN}\,|\,kl\rangle}{D_{ijab}D_{klab}}$$

involved partial-wave decomposition

$$\frac{E^{(3)}_{ph}}{V} = +\sum_{\substack{abc\\ijk}}\frac{\langle ij\,|\,\overline{V}_{\rm NN}\,|\,ab\rangle\langle ak\,|\,\overline{V}_{\rm NN}\,|\,ic\rangle\langle bc\,|\,\overline{V}_{\rm NN}\,|\,jk\rangle}{D_{ijab}D_{jkbc}}$$

see Coraggio, Holt *et al.*, PRC **89**, 044321

$$\frac{E^{(3)}_{pp}}{V} = +\frac{1}{8}\sum_{\substack{abcd\\ij}}\frac{\langle ij\,|\,\overline{V}_{\rm NN}\,|\,ab\rangle\langle ab\,|\,\overline{V}_{\rm NN}\,|\,cd\rangle\langle cd\,|\,\overline{V}_{\rm NN}\,|\,ij\rangle}{D_{ijab}D_{ijcd}}$$

third order

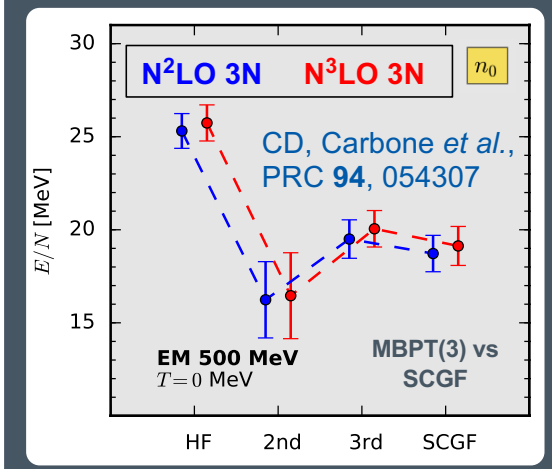

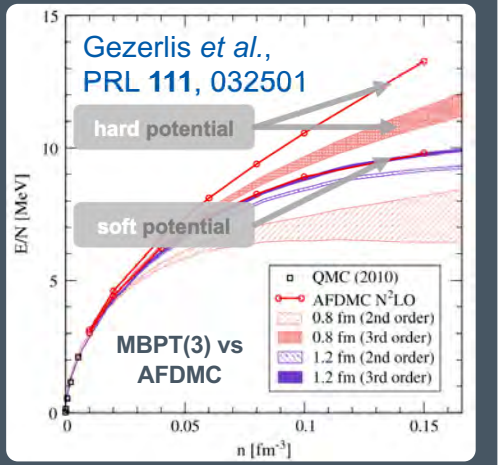

nonperturbative benchmarks in neutron matter

Example: second-order contribution

OHIO UNIVERSITY

$$\frac{E^{(2)}_{\mathrm{NN+\overline{3N}}}}{V} = \frac{1}{4}\prod_{i=1}^{4}\left[\mathrm{Tr}_{\sigma_i}\mathrm{Tr}_{\tau_i}\int\frac{\mathrm{d}\mathbf{k}_i}{(2\pi)^3}\right]\left|\left\langle 12\left|V^{(2)}_{\mathrm{as}}\right|34\right\rangle\right|^2 \frac{n^{\tau_1}_{\mathbf{k}_1} n^{\tau_2}_{\mathbf{k}_2}(1-n^{\tau_3}_{\mathbf{k}_3})(1-n^{\tau_4}_{\mathbf{k}_4})}{\varepsilon^{\tau_1}_{\mathbf{k}_1}+\varepsilon^{\tau_2}_{\mathbf{k}_2}-\varepsilon^{\tau_3}_{\mathbf{k}_3}-\varepsilon^{\tau_4}_{\mathbf{k}_4}}$$

$$|i\rangle = |\mathbf{k}_i\sigma_i\tau_i\rangle$$

Partial-wave method (spin sums)

$$\sum_{S,M_S,M'_S}\left|\langle \mathbf{k}\,SM_S\,|\,V^{(2)}_{\mathrm{as}}\,|\,\mathbf{k}'\,SM'_S\rangle\right|^2 = \sum_L P_L(\cos\theta_{\mathbf{k},\mathbf{k}'})$$

$$\times \sum_{J,l,l',S}\sum_{\widetilde{J},\widetilde{l},\widetilde{l}'}(4\pi)^2\, i^{(l-l'+\widetilde{l}-\widetilde{l}')}\,(-1)^{\widetilde{l}+l'+L}\,\mathcal{C}^{L0}_{l0\widetilde{l}'0}\,\mathcal{C}^{L0}_{l'0\widetilde{l}0}$$

$$\times \sqrt{(2l+1)(2l'+1)(2\widetilde{l}+1)(2\widetilde{l}'+1)}\,(2J+1)(2\widetilde{J}+1)$$

$$\times \begin{Bmatrix} l & S & J \\ \widetilde{J} & L & \widetilde{l}' \end{Bmatrix}\begin{Bmatrix} J & S & l' \\ \widetilde{l} & L & \widetilde{J} \end{Bmatrix}\langle k|V^{(2)}_{Sl'lJ}|k'\rangle\,\langle k'|V^{(2)}_{S\widetilde{l}'\widetilde{l}\widetilde{J}}|k\rangle$$

$$\times \left(1-(-1)^{l+S+1}\right)\left(1-(-1)^{\widetilde{l}+S+1}\right),$$

special case: PNM (no isospin terms)

Tolos, Friman, Schwenk, NPA **806** 105

- previous approach: manual partial-wave decomposition of each diagram: **tedious & error-prone**, especially in ANM
- Instead: perform MBPT calculations directly in a single-particle basis

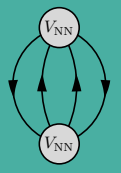

$$\frac{E^{(2)}}{V} = \frac{1}{4}\sum_{\substack{ij\\ab}}\frac{|\langle ij|\overline{V}_{\mathrm{NN}}|ab\rangle|^2}{\varepsilon_i+\varepsilon_j-\varepsilon_a-\varepsilon_b}$$

second order

Alternative avenue: Automated Momentum Coupling (AMC)
Tichai, Wirth et al., EPJ A **56**, 272; https://github.com/radnut/amc

Example: second-order contribution

OHIO UNIVERSITY

$$\frac{E^{(2)}_{\mathrm{NN+3N}}}{V} = \frac{1}{4}\prod_{i=1}^{4}\left[\mathrm{Tr}_{\sigma_i}\mathrm{Tr}_{\tau_i}\int\frac{\mathrm{d}\mathbf{k}_i}{(2\pi)^3}\right]\left|\left\langle 12\left|V^{(2)}_{\mathrm{as}}\right|34\right\rangle\right|^2 \frac{n^{\tau_1}_{\mathbf{k}_1} n^{\tau_2}_{\mathbf{k}_2}(1-n^{\tau_3}_{\mathbf{k}_3})(1-n^{\tau_4}_{\mathbf{k}_4})}{\varepsilon^{\tau_1}_{\mathbf{k}_1}+\varepsilon^{\tau_2}_{\mathbf{k}_2}-\varepsilon^{\tau_3}_{\mathbf{k}_3}-\varepsilon^{\tau_4}_{\mathbf{k}_4}}$$

$$|i\rangle = |\mathbf{k}_i\sigma_i\tau_i\rangle$$

Partial-wave method (spin sums)

$$\sum_{S,M_S,M'_S}\left|\langle \mathbf{k}\,SM_S\,|\,V^{(2)}_{\mathrm{as}}\,|\,\mathbf{k}'\,SM'_S\rangle\right|^2 = \sum_L P_L(\cos\theta_{\mathbf{k},\mathbf{k}'})$$

$$\times \sum_{J,l,l',S}\sum_{\tilde{J},\tilde{l},\tilde{l}'}(4\pi)^2\, i^{(l-l'+\tilde{l}-\tilde{l}')}\,(-1)^{\tilde{l}+l'+L}\,\mathcal{C}^{L0}_{l0\tilde{l}'0}\,\mathcal{C}^{L0}_{l'0\tilde{l}0}$$

$$\times \sqrt{(2l+1)(2l'+1)(2\tilde{l}+1)(2\tilde{l}'+1)}\,(2J+1)(2\tilde{J}+1)$$

$$\times \begin{Bmatrix} l & S & J \\ \tilde{J} & L & \tilde{l}' \end{Bmatrix}\begin{Bmatrix} J & S & l' \\ \tilde{l} & L & \tilde{J} \end{Bmatrix}\langle k|V^{(2)}_{Sl'\tilde{l}J}|k'\rangle\,\langle k'|V^{(2)}_{S\tilde{l}'\tilde{l}J}|k\rangle$$

$$\times (1-$$

See also Alexander Tichai's talk:
Symmetry reduction of tensor networks in many-body theory

- previous approach: manual partial-wave decomposition of each diagram: **tedious & error-prone**, especially in ANM
- Instead: perform MBPT calculations directly in a single-particle basis

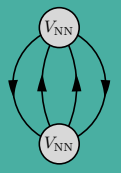

$$\frac{E^{(2)}}{V} = \frac{1}{4}\sum_{\substack{ij\\ab}}\frac{|\langle ij|\overline{V}_{\mathrm{NN}}|ab\rangle|^2}{\varepsilon_i+\varepsilon_j-\varepsilon_a-\varepsilon_b}$$

second order

Alternative avenue: Automated Momentum Coupling (AMC)
Tichai, Wirth et al., EPJ A **56**, 272; https://github.com/radnut/amc

Many-body interactions

CD, Hebeler, Schwenk, PRL **122**, 042501

OHIO UNIVERSITY

$$\langle 1'2'\ldots A' \,|\, \mathcal{A}_A V_{\rm AN} \,|\, 12\ldots A\rangle = \langle (\sigma_{1'}\tau_{1'})\ldots(\sigma_{A'}\tau_{A'}) \,|\, \mathcal{A}_A V_{\rm AN}\,(\overline{\mathbf{p}},\overline{\mathbf{p}}') \,|\, (\sigma_1\tau_1)\ldots(\sigma_A\tau_A)\rangle$$

(binary number) (binary number)

complex-valued, antisymmetrized

3*A*-dimensional momenta

$$\overline{\mathbf{p}} = \mathbf{p}_1 \oplus \mathbf{p}_2 \ldots \oplus \mathbf{p}_A \quad (\text{similar for } \overline{\mathbf{p}}')$$

$$\boldsymbol{\sigma}_i^{(j)} = (\mathbb{1}_2\otimes\mathbb{1}_2)_1 \otimes\ldots\otimes \left(\boldsymbol{\sigma}_i^{(j)}\otimes\mathbb{1}_2\right)_i \otimes\ldots\otimes(\mathbb{1}_2\otimes\mathbb{1}_2)_A$$

$$\boldsymbol{\tau}_i^{(j)} = (\mathbb{1}_2\otimes\mathbb{1}_2)_1 \otimes\ldots\otimes \left(\mathbb{1}_2\otimes\boldsymbol{\tau}_i^{(j)}\right)_i \otimes\ldots\otimes(\mathbb{1}_2\otimes\mathbb{1}_2)_A$$

$$\mathbf{p}_i^{(j)} = (\mathbb{1}_2\otimes\mathbb{1}_2)_1 \otimes\ldots\otimes(\mathbb{1}_2\otimes\mathbb{1}_2)_i\ \mathbf{p}_i^{(j)} \otimes\ldots\otimes(\mathbb{1}_2\otimes\mathbb{1}_2)_A = \mathbf{p}_i^{(j)}\,\mathbb{1}_A\,,$$

Pauli matrices (for spin/isospin)

A	4^A
2	16
3	64
4	256

(sparse) $4^A \times 4^A$ Matrices

Only $4^A \binom{2A}{A}$ **are nonzero!**

represent interactions as matrices **in spin-isospin space**

- automated generation (via *symbolic* calculations) using analytic expressions: **NN**, **3N**, **4N** forces up to N^{3}LO implemented
- matrix elements are analytic functions of the single-particle momenta, written in C^{++} (no approximations involved)
- (Physics-based) optimization (symmetries, common subexpr., …)

$$\mathcal{A}_A = \sum_{a=1}^{A!} \mathrm{sign}(\pi_a)\, P_{\pi_a}$$

momentum spin isospin

(likewise for isospin) $P_{ij}^{\rm spin} = \dfrac{\mathbb{1} + \boldsymbol{\sigma}_i\cdot\boldsymbol{\sigma}_j}{2}$

Many-body interactions

CD, Hebeler, Schwenk, PRL **122**, 042501

OHIO UNIVERSITY

$$\langle 1'2'\ldots A' \,|\, \mathcal{A}_A V_{\rm AN} \,|\, 12\ldots A\rangle = \langle (\sigma_{1'}\tau_{1'})\ldots(\sigma_{A'}\tau_{A'}) \,|\, \mathcal{A}_A V_{\rm AN}\,(\overline{\mathbf{p}},\overline{\mathbf{p}}') \,|\, (\sigma_1\tau_1)\ldots(\sigma_A\tau_A)\rangle$$

complex-valued, antisymmetrized

3*A*-dimensional momenta

$$\overline{\mathbf{p}} = \mathbf{p}_1 \oplus \mathbf{p}_2 \ldots \oplus \mathbf{p}_A$$

(similar for $\overline{\mathbf{p}}'$)

Illustrative example #1:

$$|\eta\rangle := |(\sigma_1\tau_1)(\sigma_2\tau_2)\ldots(\sigma_A\tau_A)\rangle$$

(ignore spin for brevity)

$$\langle \eta' \,|\, \boldsymbol{\tau}_1\cdot\boldsymbol{\tau}_2 \,|\, \eta\rangle = \sum_{j=1}^{3} \tau_1^{(j)} \otimes \tau_2^{(j)} = \begin{pmatrix} 1 & 0 & 0 & 0 \\ 0 & -1 & 2 & 0 \\ 0 & 2 & -1 & 0 \\ 0 & 0 & 0 & 1 \end{pmatrix}$$

$$\nu_1^{(\lambda=1)} = \begin{pmatrix} 1 \\ 0 \\ 0 \\ 0 \end{pmatrix}, \quad \nu_2^{(\lambda=1)} = \frac{1}{\sqrt{2}}\begin{pmatrix} 0 \\ 1 \\ 1 \\ 0 \end{pmatrix}, \quad \nu_3^{(\lambda=1)} = \begin{pmatrix} 0 \\ 0 \\ 0 \\ 1 \end{pmatrix},$$

and $\quad \nu_4^{(\lambda=-3)} = \frac{1}{\sqrt{2}}\begin{pmatrix} 0 \\ 1 \\ -1 \\ 0 \end{pmatrix}$

We identify the isospin *singlet* and *triplet* *states* with eigenvalues $\lambda = (2T(T+1) - 3)$

Many-body interactions

CD, Hebeler, Schwenk, PRL **122**, 042501

OHIO UNIVERSITY

$$\langle 1'2'\ldots A' \,|\, \mathcal{A}_A V_{\rm AN} \,|\, 12\ldots A\rangle = \langle (\sigma_{1'}\tau_{1'})\ldots(\sigma_{A'}\tau_{A'}) \,|\, \mathcal{A}_A V_{\rm AN}\,(\overline{\mathbf{p}},\overline{\mathbf{p}}') \,|\, (\sigma_1\tau_1)\ldots(\sigma_A\tau_A)\rangle$$

complex-valued, antisymmetrized

3*A*-dimensional momenta

$$\overline{\mathbf{p}} = \mathbf{p}_1 \oplus \mathbf{p}_2 \ldots \oplus \mathbf{p}_A$$

(similar for $\overline{\mathbf{p}}'$)

Illustrative example #2:

(ignore isospin for brevity)

$$|\eta\rangle := |(\sigma_1\tau_1)(\sigma_2\tau_2)\ldots(\sigma_A\tau_A)\rangle$$

$$\langle \eta' \,|\, \boldsymbol{\sigma}_1\cdot\mathbf{q}\,\boldsymbol{\sigma}_2\cdot\mathbf{q} \,|\, \eta\rangle = \sum_{i,j=1}^{3} \left[\sigma_1^{(i)} \otimes \left(q_{(i)}\mathbb{1}_2\right)\right]\left[\sigma_2^{(j)} \otimes \left(q_{(j)}\mathbb{1}_2\right)\right]$$

Hermitian

$$= \begin{pmatrix} q_{(z)}^2 & (q_{(x)} - iq_{(y)})q_{(z)} & (q_{(x)} - iq_{(y)})q_{(z)} & (q_{(x)} - iq_{(y)})^2 \\ (q_{(x)} + iq_{(y)})q_{(z)} & -q_{(z)}^2 & q_{(x)}^2 + q_{(y)}^2 & -(q_{(x)} - iq_{(y)})q_{(z)} \\ (q_{(x)} + iq_{(y)})q_{(z)} & q_{(x)}^2 + q_{(y)}^2 & -q_{(z)}^2 & -(q_{(x)} - iq_{(y)})q_{(z)} \\ (q_{(x)} + iq_{(y)})^2 & -(q_{(x)} + iq_{(y)})q_{(z)} & -(q_{(x)} + iq_{(y)})q_{(z)} & q_{(z)}^2 \end{pmatrix}$$

Efficient Monte-Carlo framework

CD, Hebeler, Schwenk, PRL **122**, 042501

OHIO UNIVERSITY

$$\langle 1'2'\ldots A' \,|\, \mathcal{A}_A V_{\rm AN} \,|\, 12\ldots A\rangle = \langle (\sigma_{1'}\tau_{1'})\ldots(\sigma_{A'}\tau_{A'}) \,|\, \mathcal{A}_A V_{\rm AN}\,(\overline{\mathbf{p}},\overline{\mathbf{p}}') \,|\, (\sigma_1\tau_1)\ldots(\sigma_A\tau_A)\rangle$$

complex-valued, antisymmetrized

3*A*-dimensional momenta

$$\overline{\mathbf{p}} = \mathbf{p}_1 \oplus \mathbf{p}_2 \ldots \oplus \mathbf{p}_A \quad (\text{similar for } \overline{\mathbf{p}}')$$

What if the analytic expressions of the interactions are *unknown*?

$$\langle (\sigma_{1'}\tau_{1'})(\sigma_{1'}\tau_{2'}) | \mathcal{A}_{12} V_{\rm NN}\,(\overline{\mathbf{p}},\overline{\mathbf{p}}') \,| (\sigma_1\tau_1)(\sigma_2\tau_2)\rangle$$

$$= (4\pi)^2 \sum_{J,L,L'} i^{L-L'} \sum_{S,T} \mathcal{C}^{Sm_S}_{1/2\sigma_1 1/2\sigma_2} \mathcal{C}^{Sm_{S'}}_{1/2\sigma_{1'} 1/2\sigma_{2'}}$$

Sum over partial waves instead

$$\times\, \mathcal{C}^{Tm_T}_{1/2\tau_1 1/2\tau_2} \mathcal{C}^{Tm_T}_{1/2\tau_{1'} 1/2\tau_{2'}}\, V^{JT}_{LL'S}(p,p')\, \left[1-(-1)^{L+S+T}\right]$$

$$\times \sum_M \mathcal{C}^{JM_J}_{LMSm_S} \mathcal{C}^{JM_J}_{L'M'Sm_{S'}} Y^{*M}_L(\theta_{\mathbf{p}},\varphi_{\mathbf{p}}) Y^{M'}_{L'}(\theta_{\mathbf{p}'},\varphi_{\mathbf{p}'})\,,$$

Rigorous UQ for nuclear matter

CD, Furnstahl, Melendez, Phillips, PRL **125**, 202702

OHIO UNIVERSITY

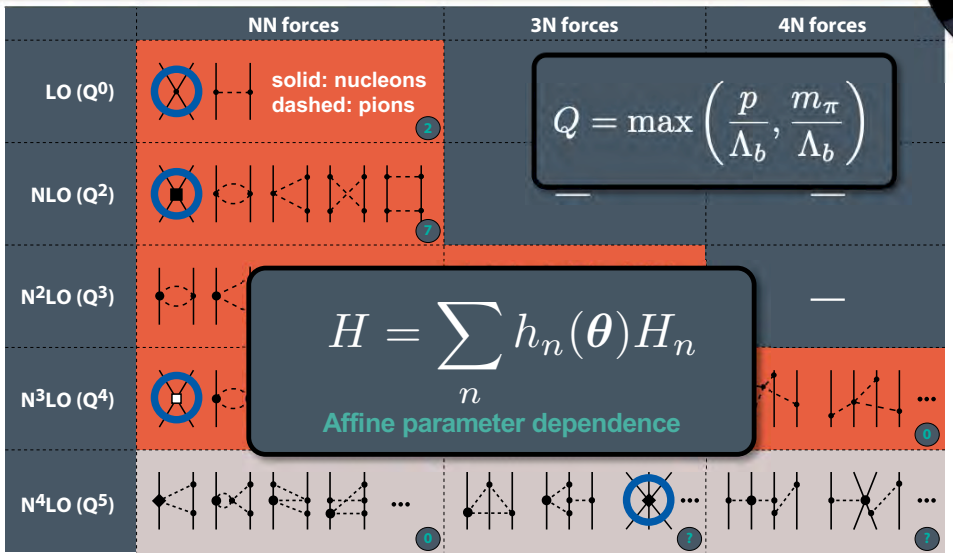

Chiral Effective Field Theory (nucleons & pions)

dominant approach for deriving *microscopic* interactions consistent with the symmetries of *low-energy* QCD

three- and four-neutron forces predicted through N^{3}LO

enables **uncertainty quantification** (EFT truncation)

fit the unknown (low-energy) couplings to experimental (or lattice) data, such as phase shifts, binding energies, charge radii, etc.

Weinberg, van Kolck, Kaplan, Savage, Wise, Epelbaum, Kaiser, Krebs, Machleidt, Meißner, ...

An example: symmetric matter

$$y = \frac{E}{A}, \quad k = 4 \quad (\mathrm{N^3LO})$$

Uncertainty bands depict 68% credibility regions

$$y = y_k + \delta y_k$$

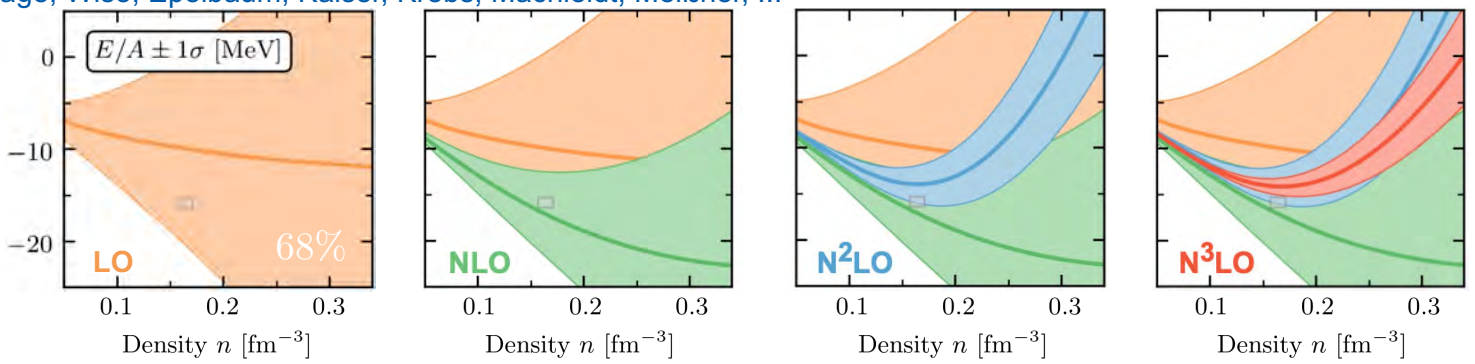

3N forces up to N^{3}LO partial-wave decomposed

OHIO UNIVERSITY

Efficient calculation of chiral three-nucleon forces up to N^{3}LO for *ab initio* studies

K. Hebeler, H. Krebs, E. Epelbaum, J. Golak, and R. Skibiński
Phys. Rev. C **91**, 044001 – Published 15 April 2015

Article | References | Citing Articles (68) | PDF | HTML | Export Citation

ABSTRACT

We present a novel framework to decompose three-nucleon forces in a momentum-space partial-wave basis. The new approach is computationally much more efficient than previous methods and opens the way to *ab initio* studies of few-nucleon scattering processes, nuclei, and nuclear matter based on higher-order chiral three-nucleon forces. We use the new framework to calculate matrix elements of chiral three-nucleon forces at next-to-next-to-leading-order and next-to-next-to-next-to-leading-order in large basis spaces and carry out benchmark calculations for neutron matter and symmetric nuclear matter. We also study the size of the individual three-nucleon-force contributions for ^{3}H. For nonlocal regulators, we find that the subleading terms, which have been neglected in most calculations so far, provide important contributions. All matrix elements are calculated and stored in a user-friendly way, such that values of low-energy constants as well as the form of regulator functions can be chosen freely.

see also: Miyagi, Stroberg *et al.*, Phys. Rev. C **105**, 014302
Hebeler, Durant *et al.*, Phys. Rev. C **107**, 024310

TABLE I. Dimension and file size of the individual 3NF matrix element files up to N^{3}LO for the different three-body partial waves. All matrix elements are calculated and stored in such a way that values of the low-energy couplings c_1, c_3, c_4, c_D, c_E, C_S, and C_T can be chosen freely for the different topologies, leading to a total of 12 files for each partial wave (see main text). For all partial waves $N_p = N_q = 15$ has been used. N_α denotes the number of partial-wave channels defined in Eq. (8). All given values apply to both three-body parities.

$\mathcal{J}$	$\mathcal{T}$	$J_{\max}$	N_α	File size [GB]
1/2	1/2	8	66	0.8
3/2	1/2	8	126	3.0
5/2	1/2	8	178	6.0
7/2	1/2	7	190	6.8
9/2	1/2	6	178	6.0
1/2	3/2	8	34	0.2
3/2	3/2	8	65	0.8
5/2	3/2	8	92	1.6
7/2	3/2	7	91	1.6
9/2	3/2	6	94	1.7

$$|pq\alpha\rangle \equiv |pq;[(LS)J(ls)j]\,\mathcal{J}(Tt)\mathcal{T}\rangle\ , \qquad (8)$$

Renaissance of MBPT

CD, Hebeler, Schwenk, PRL **122**, 042501
CD, McElvain *et al.*, in prep.

OHIO UNIVERSITY

Efficient evaluation of MBPT diagrams

with **NN**, **3N**, and **4N forces**

- **implementation of arbitrary diagrams** has become **straightforward** (up to numerical precision)
- multi-dimensional momentum integrals: improved Vegas
- **GPU-accelerated normal ordering** of 3N interactions
- propagation of importance sampling distributions
- **controlled evaluation of 1000s of MBPT diagrams**
- **acceleration: MPI + openMP + GPU (CUDA)**

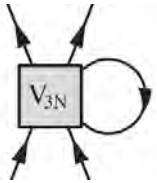

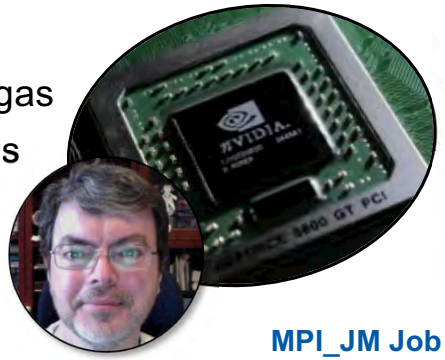

high-order MBPT calculations of the EOS

automated code generation

analytic expressions
interaction & MBPT diagrams

Application to dilute Fermi gas:
Wellenhofer, CD, Schwenk, PRC **104**, 014003 & PLB **802**, 135247

MPI_JM Job Manager:
Berkowitz, Jansen, **McElvain**, and Walker-Loud,
EPJ Web Conf. **175**, 09007 (2018 Gordon Bell finalists)

(Rule-based) Automated Code Generation

OHIO UNIVERSITY

$$\frac{E^{(3)}_{ph}}{V} = +\sum_{\substack{abc\\ijk}} \frac{\langle ij\,|\,\overline{V}_{\rm NN}\,|\,ab\rangle\,\langle ak\,|\,\overline{V}_{\rm NN}\,|\,ic\rangle\,\langle bc\,|\,\overline{V}_{\rm NN}\,|\,jk\rangle}{D_{ijab}D_{jkbc}}$$

an example: third order ph diagram

(inverse) factor $F = +1\,,$

numerator $V = \{\{a,b,i,j\},\{i,c,a,k\},\{j,k,b,c\}\}\,,$

denominator $D = \{\{i,j,a,b\},\{j,k,b,c\}\}$

Derive the MBPT diagram of interest and its corresponding analytic expression

Determine labels determined by momentum conservation
Generate LaTeX output for documentation

Check internal consistency of the analytic expression;
Do the vertices conserve momentum?

Trust but verify (spot check some of the diagrams)
Run code generator and compile the output

Evaluate diagram for a given (*n*, *x*, *T*) and Hamiltonian and store the result in a database

repeat for each diagram (embarrassingly parallel)

$$\{a,b,c,i,j,k\}$$

$$\begin{aligned}
\mathbf{p}_a + \mathbf{p}_b &= \mathbf{p}_i + \mathbf{p}_j\,,\\
\mathbf{p}_i + \mathbf{p}_c &= \mathbf{p}_a + \mathbf{p}_k\,,\\
\mathbf{p}_j + \mathbf{p}_k &= \mathbf{p}_b + \mathbf{p}_c\,,
\end{aligned}$$

Momentum conservation determines *N* – 1 momenta in MBPT(*N*)

Symbolic integration reduces dimensionality of the integrals

Choose one configuration:

$$\begin{aligned}
b &= -a+i+j\\
c &= a-i+k
\end{aligned}$$

Offline-online decomposition

(Rule-based) Automated Code Generation

OHIO UNIVERSITY

$$\frac{E_{ph}^{(3)}}{V} = +\sum_{\substack{abc\\ijk}} \frac{\langle ij\,|\,\overline{V}_{\rm NN}\,|\,ab\rangle\,\langle ak\,|\,\overline{V}_{\rm NN}\,|\,ic\rangle\,\langle bc\,|\,\overline{V}_{\rm NN}\,|\,jk\rangle}{D_{ijab}D_{jkbc}}$$

an example: third order ph diagram

- Set up integrator (Integrate over all *particle* & *hole* labels not determined by momentum conservation)
- Perform variable transforms (to Cartesian momenta)
- Use momentum conservation to determine momenta not integrated over and assign momenta to all vertices
- Pre-store all interaction matrices (including those with normal ordering) and single-particle energies
- Contract the interaction matrices (weighted by the energy denominator) and multiply by overall factor

(inverse) factor $F = +1\,,$

numerator $V = \{\{a,b,i,j\},\{i,c,a,k\},\{j,k,b,c\}\}\,,$

denominator $D = \{\{i,j,a,b\},\{j,k,b,c\}\}$

Holes: inside the Fermi sphere (T = 0)
Particles: outside the Fermi sphere $\{a,i,j,k\}$

Use spherical coordinates due to momentum distribution functions, *e.g.*, $n_{\boldsymbol{p}} = \vartheta(\, k_{\rm F} - |\, \boldsymbol{p}\,|\,)$

$$b = -a+i+j$$
$$c = a-i+k$$

Gauss-Legendre Lebedev quadrature

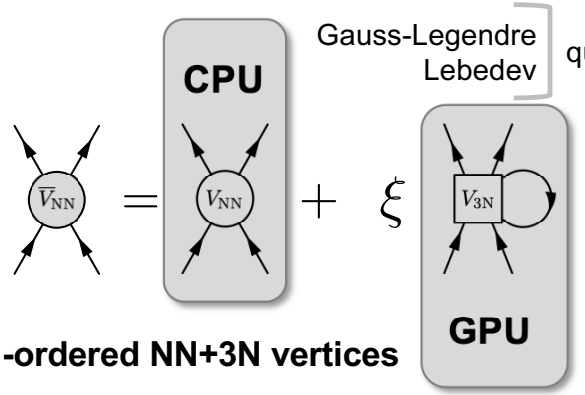

normal-ordered NN+3N vertices

High-order MBPT for nuclear matter

OHIO UNIVERSITY

General paradigm:
evaluate all diagrams consistently
or none at all

The number of diagrams increases rapidly!

n =	2	3	4	5	6	7
	1,	3,	39,	840,	27 300,	1 232 280, …

Integer sequence A064732:
Number of labeled Hugenholtz diagrams with *n* nodes.

See also Pierre Arthuis's talk:
Automated generation and evaluation of diagrams at play in various many-body methods

with automated diagram generation

Stevenson, Int. J. Mod. Phys. C **14**, 1135
Arthuis *et al.*, Comput. Phys. **240**, 202

first automated approach to MBPT for nuclear matter

for residual 3N contributions, see Xu, Li, and Xu, arXiv:1810.08804

Implementing 3N interactions

Bogner *et al.*, Prog. Part. Nucl. Phys. **65**
Hergert *et al.*, Phys. Rep. **621**, 165

OHIO UNIVERSITY

Normal-ordering w.r.t. a finite-density reference state. Here: HF reference state.

General three-body Hamiltonian in second-quantized form:

$$H = \sum_{12} T_{12} a_1^\dagger a_2 + \frac{1}{(2!)^2} \sum_{1234} \langle 12|V|34\rangle a_1^\dagger a_2^\dagger a_4 a_3 + \frac{1}{(3!)^2} \sum_{123456} \langle 123|V^{(3)}|456\rangle a_1^\dagger a_2^\dagger a_3^\dagger a_6 a_5 a_4$$

all operators are normal-ordered w.r.t. the vacuum

$$H = E_0 + \sum_{12} f_{12}\{a_1^\dagger a_2\} + \frac{1}{(2!)^2} \sum_{1234} \langle 12|\Gamma|34\rangle \{a_1^\dagger a_2^\dagger a_4 a_3\} + \frac{1}{(3!)^2} \sum_{123456} \langle 123|\Gamma^{(3)}|456\rangle \{a_1^\dagger a_2^\dagger a_3^\dagger a_6 a_5 a_4\}$$

where the zero-, one-, and two-body normal-ordered terms are given by

$$\langle\Phi|H|\Phi\rangle = \sum_1 T_{11} n_1 + \frac{1}{2} \sum_{12} \langle 12|V|12\rangle n_1 n_2 + \frac{1}{3!} \sum_{123} \langle 123|V^{(3)}|123\rangle n_1 n_2 n_3 ,$$

$$T_{12} + \sum_i \langle 1i|V|2i\rangle n_i + \frac{1}{2} \sum_{ij} \langle 1ij|W|2ij\rangle n_i n_j , \qquad n_i = \theta(\varepsilon_F - \varepsilon_i)$$

$$\langle 12|\Gamma|34\rangle = \langle 12|V|34\rangle + \sum_i \langle 12i|V^{(3)}|34i\rangle n_i ,$$

density-dependent two-body potential

Use **Wick's theorem** to rewrite the ge… exact…

Trunc… normal ordered two-body level includes **(dominant) 3N contributions**

See also Matthias Heinz's talk:
Diagrammatic resummations for the IMSRG method

Normal-ordered 3N Hamiltonian

Roth *et al.* (CC calculations), Phys. Rev. Lett. **109**, 052501 (2012)

OHIO UNIVERSITY

Normal ordering shifts contributions from the three-body Hamiltonian operator to effective lower-body operators plus a residual (reduced) three-body operator.

$$\langle 12|\Gamma|34\rangle = \langle 12|V|34\rangle + \sum_i \langle 12i|V^{(3)}|34i\rangle n_i \,,$$

Density-dependent (effective) two-body potential

$$\left\langle \mathbf{2'3'} \left| V_{\rm NN}^{\rm med} \right| \mathbf{23} \right\rangle = \bar{V}_{\rm 3N} = \sum_{\sigma_1\tau_1} \int \frac{\mathrm{d}\mathbf{k}_1}{(2\pi)^3} f_1 \left\langle \mathbf{12'3'} \left| \bar{V}_{\rm 3N} \right| \mathbf{123} \right\rangle$$

Its matrix elements are obtained by summing one particle over the occupied states in the reference state

for residual 3N contributions, see Xu, Li, and Xu, arXiv:1810.08804

Hence, a many-body framework built only for NN interactions can then incorporate a **density-dependent effective two-body potential** derived from 3N forces by replacing:

$$V_{\rm NN} \to V_{\rm NN} + \xi\, V_{\rm NN}^{\rm med}$$

The combinatorial factor ξ is determined by Wick's theorem and depends on the many-body calculation of interest.

Normal ordering has become the standard approach to implementing (dominant) 3N contributions in *ab initio* many-body calculations.

with the shorthand notation $|i\rangle = |\mathbf{k}_i\sigma_i\tau_i\rangle$, antisymmetrized 3N interactions $\bar{V}_{\rm 3N}$, and momentum distribution function of the reference state f_1.

Common approximations

For nuclei, *e.g.*, see Roth *et al.*, Phys. Rev. Lett. **109**, 052501 (2012)

OHIO UNIVERSITY

#1 In contrast to the (Galilean-invariant) NN potential, the effective two-body potential depends on the center-of-mass momentum ***P*** of the two remaining particles.

Hence, **both potentials *cannot* be straightforwardly combined in a partial-wave basis.**

Different approximations for the ***P*** dependence have been used to enable applications to nuclear matter.

Automated MBPT does *not* require any of these approximations.

$$\left\langle 2'3' \left| V_{\rm NN}^{\rm med} \right| 23 \right\rangle = \bar{V}_{\rm 3N} \;(P) = \sum_{\sigma_1\tau_1} \int \frac{{\rm d}k_1}{(2\pi)^3} f_1 \left\langle 12'3' \left| \bar{V}_{\rm 3N} \right| 123 \right\rangle$$

Available at arbitrary proton fractions, densities, and temperatures based on different 3N interactions (up to N^{3}LO+)

semi-analytic calculations: ***P* = 0**
PW-based calculations: **average over all angles of *P***

How accurate are these approximations?

Errors of two approximations for the 3N HF energy as a function of the density $n = n_p + n_n$

What about higher orders?

with the proton fraction $x = n_p/n$ of **infinite nuclear matter**

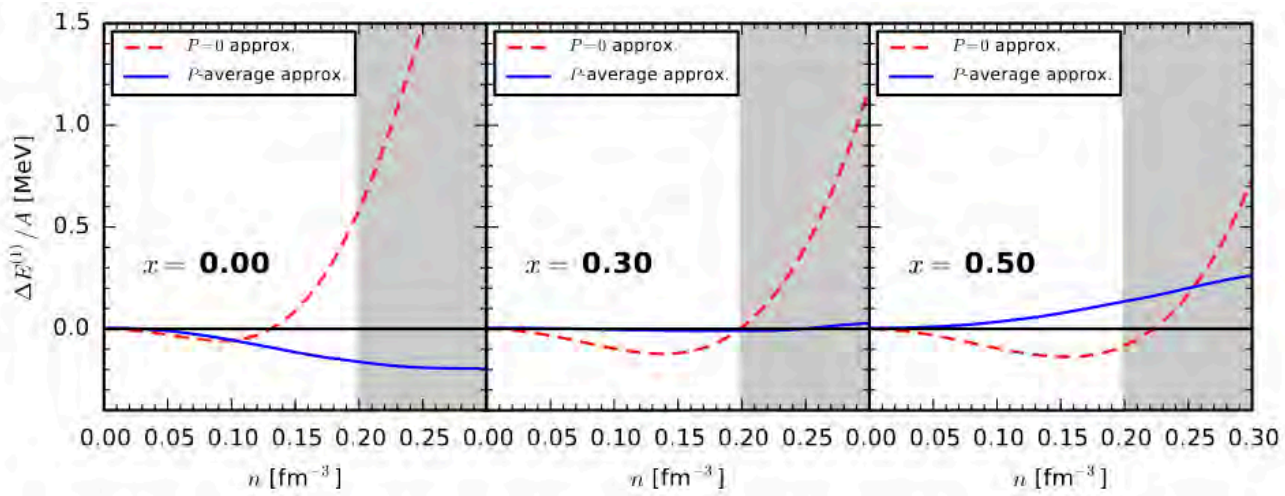

Drischler, Hebeler, and Schwenk, Phys. Rev. C **93**, 054314

Residual 3N contributions

OHIO UNIVERSITY

#2 The three-body term in the normal-ordered Hamiltonian *cannot* be implemented using effective two-body potentials.

These ***residual 3N contributions*** have been studied in CC and MBPT (Kaiser, Hagen *et al.*, CD *et al.*)

They are expected to be smaller than EFT truncation error (and other MBPT diagrams at the same order)

They are relatively inexpensive to evaluate using automated MBPT.

$$\mathcal{E}_2^{\rm res}(k_{\rm F}) = \quad = -\frac{1}{36}\sum_{ijkabc} V^{ijk,abc}V^{abc,ijk}f_{ijk}\bar{f}_{abc}\frac{1}{D_{abc,ijk}},$$

Residual third-order terms were first studied in closed-shell nuclei: from ^{4}He to ^{48}Ca by Hu, Li, and Xu, arXiv:1810.08804

For relevant references, see Section 2.5 in:
CD, Holt, and Wellenhofer, ARNPS **71**, 403

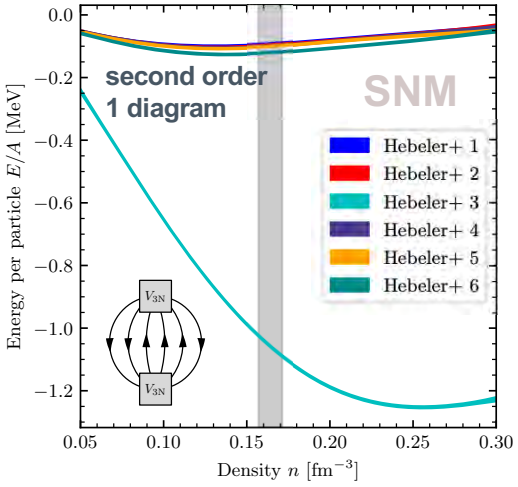

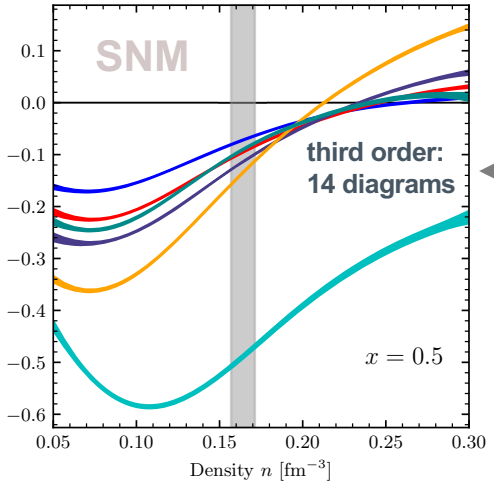

one, two, or three 3N vertices

Typically small, but hints of large cutoff dependence

Not small compared to second order. Negligible?

(work in progress)

High-order MBPT for nuclear matter

OHIO UNIVERSITY

level	MBPT(n)	N_{diag}[a]	$N_{\text{diag}}^{(\text{eff})}$	N_{dim}
two body	HF	1	1	6
	2	1	1	9
	3	3	3	18
	4	39	24	24
	5	840	375	30
	6	27300	11269	36
three body	2	1	1	18
	3	14[b]	14	21; 24; 27

(effective) dimensionality of momentum integrals. Accounts for:

- **momentum conservation**
- **rotational invariance**

MC integration algorithms include:

- **Vegas (traditional | enhanced)**
- **FOAM**
- **Importance sampling using normalizing flows** Brady *et al.*, Phys. Rev. Lett. **127**, 062701

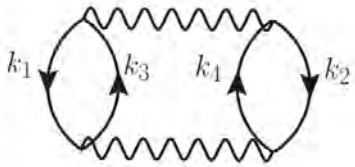

(c) (2,normal)

(effective) number of diagrams to be computed. Accounts for:

- **complex conjugated pairs**
- **anomalous diagrams**

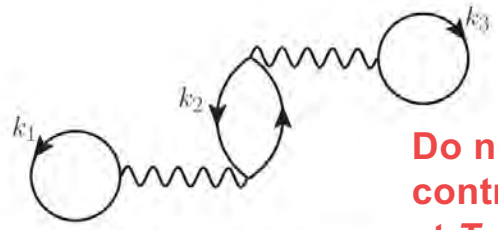

(d) (2,anomalous)

Do not contribute at $T = 0$

Wellenhofer, Holt *et al.*, PRC **89**, 064009
Keller *et al.*, PRC **103**, 055806

MBPT: an HPC application

MBPT(5)

first complete third-order calculation

propagation of importance sampling distributions

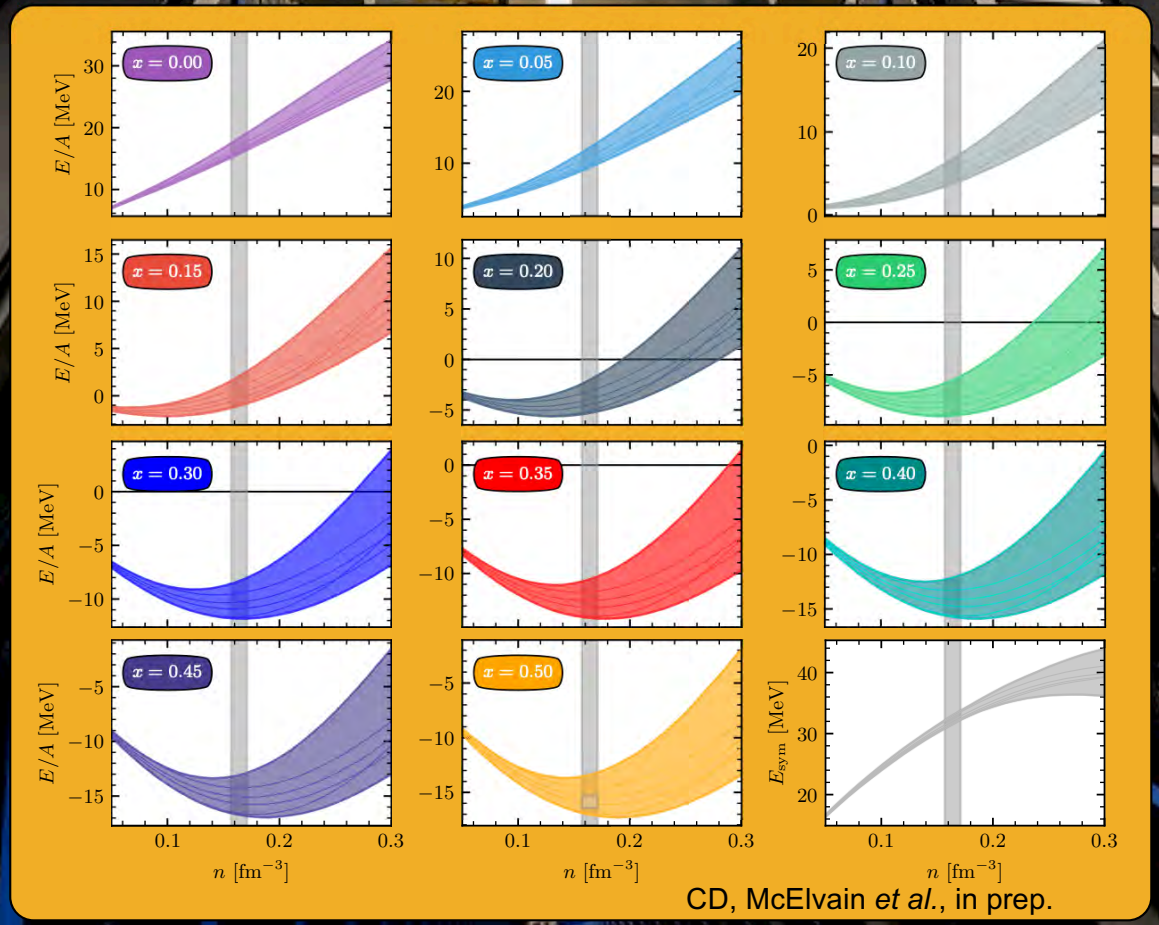

CD, McElvain *et al.*, in prep.

#5 (U.S.)

Summit @ Oak Ridge Leadership Computing Facility

202 752 CPU Cores
27 648 Nvidia GPUs
122.3 peta flops

How well do we know the *saturation point*?

CD, McElvain *et al.*, in prep.

OHIO UNIVERSITY

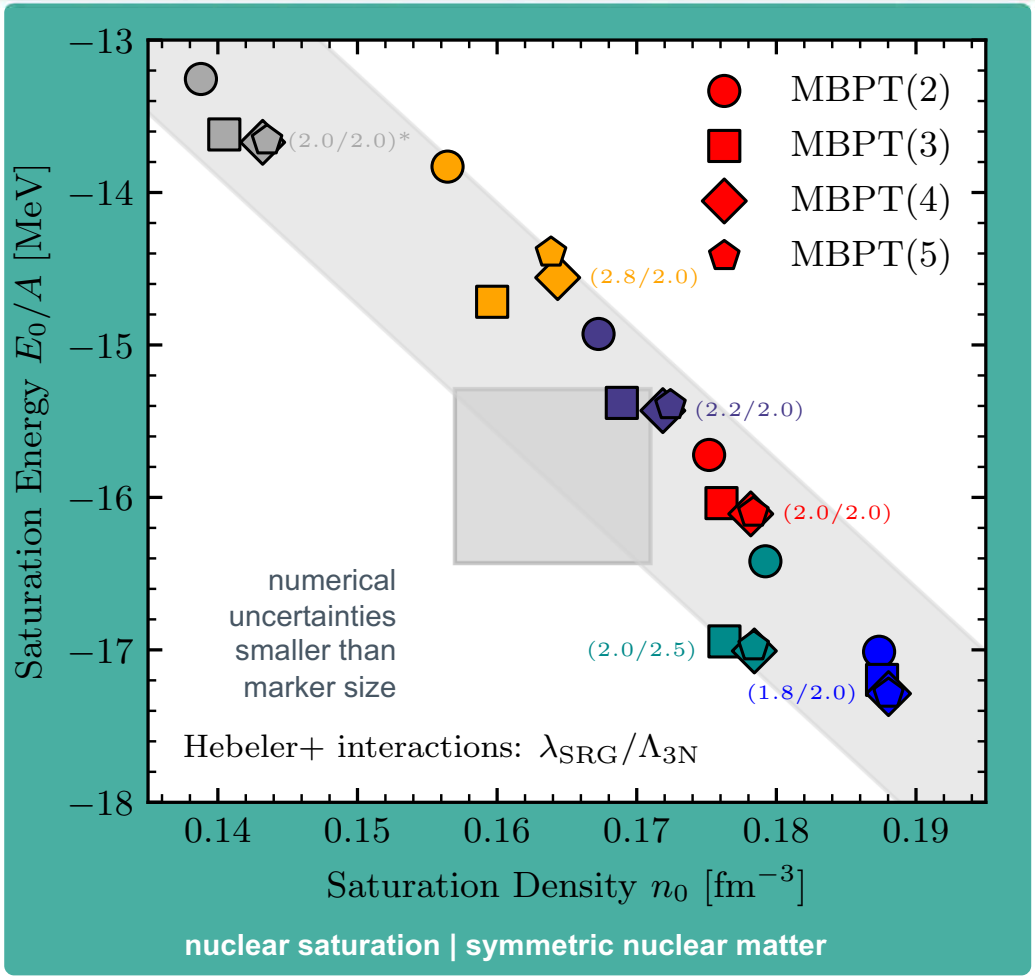

nuclear saturation | symmetric nuclear matter

MBPT(*n*)	2	3	4	5
NN+3N norm. ord.	✓	✓	✓	✓
(new) residual 3N	✓ (1)	✓ (14)	✗	✗

✓ PRL (2019) ✓ new ✗ not planned

Remarkable many-body convergence for these soft(ened) chiral NN+3N interactions

Empirical saturation point (gray box) typically not well reproduced by these chiral interactions

Many challenges were overcome!

CD, Hebeler, Schwenk, PRL **122**, 042501

OHIO UNIVERSITY

- **Higher orders: particle-hole contributions**
  Coraggio *et al.*, PRC **89**, 044321; Holt, Kaiser, PRC **95**, 034326
- **Approximated normal-ordering**
  Holt *et al.*, PRC **81**, 024002; Hebeler, Schwenk, PRC **82**, 014314
- **Neglected residual 3N diagrams**
  Hagen *et al.*, PRC **89**, 014319; Kaiser, EPJ A **48**, 58
- **Higher many-body forces**
  Hebeler *et al.*, PRC **91**, 044001

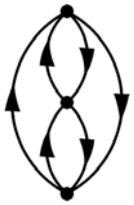

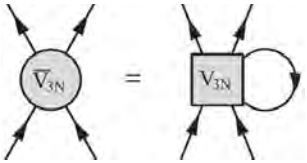

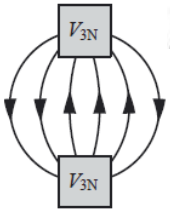

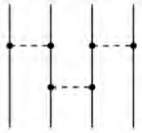

Automated Monte Carlo framework for MBPT

(Pionless) Effective field theory

Wellenhofer, CD, and Schwenk,
PRC **104**, 014003 and PLB **802**, 135247

OHIO UNIVERSITY

apply many-body perturbation theory $\frac{E^{(n)}}{E_0} \propto k_{\rm F}^n$

$$\langle \boldsymbol{p}'|V_{\rm NN}|\boldsymbol{p}\rangle = \left[C_0(\Lambda) + C_2(\Lambda)\,\frac{\boldsymbol{p}'^2+\boldsymbol{p}^2}{2} + C_2'(\Lambda)\,\boldsymbol{p}'\cdot\boldsymbol{p} + \ldots\right] \times \theta(\Lambda-p)\,\theta(\Lambda-p')$$

$$\langle \boldsymbol{p}'\boldsymbol{q}'|V_{\rm 3N}|\boldsymbol{p}\boldsymbol{q}'\rangle = \left[D_0(\Lambda) + \ldots\right] \times \theta(\Lambda-p)\,\theta(\Lambda-p')\theta(\Lambda-q)\,\theta(\Lambda-q')$$

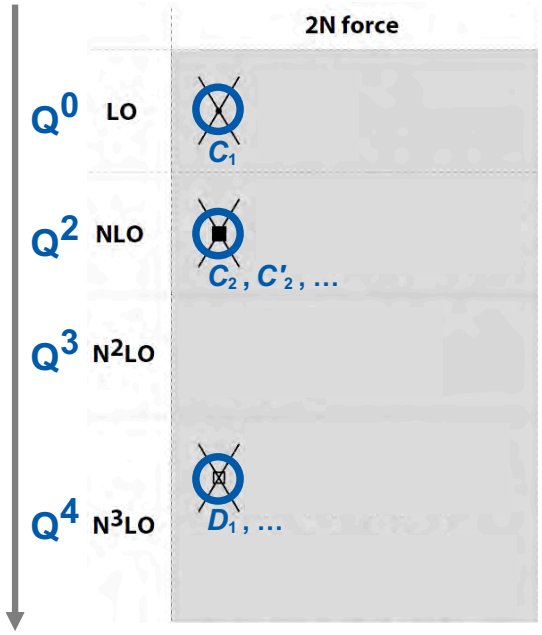

match LECs to effective-range expansion

$$C_0 = \frac{4\pi a_s}{M} \qquad C_2 = C_0\frac{a_s r_s}{2} \qquad C_2' = \frac{4\pi a_p^3}{M}$$

e.g., $\mathcal{I}_{\rm MBPT} \sim \int_0^{\Lambda} dq\,\frac{q^2}{q^2-p^2}$

renormalize LECs perturbatively to cancel divergences: Λ → ∞

Fermi-momentum expansion for the ground-state energy density

$$E(k_{\rm F}) \simeq n\frac{k_{\rm F}^2}{2M}\left[\frac{3}{5} + (g-1)\sum_{n=1}^{\infty}\mathcal{C}_n(k_{\rm F})\right]$$

Hammer, Furnstahl, Nucl. Phys. A **678**, 277
Kaplan, Savage, Wise, Nucl. Phys. B **534**, 329

$k_F\, a_s$ – expansion for the ground-state energy

OHIO UNIVERSITY

$$E(k_F) \simeq \varrho \frac{k_F^2}{2M}\Big[\underbrace{\frac{3}{5}}_{0} + \underbrace{(g-1)\Big\{\frac{2}{3\pi}k_F a_s}_{1} + \underbrace{\frac{4}{35\pi^2}(11-2\ln 2)(k_F a_s)^2}_{2} + \big(0.0755732 + 0.0573879(g-3)\big)(k_F a_s)^3\Big\} + \frac{1}{10\pi}(g-1)(k_F a_s)^2 k_F r_s + \frac{1}{5\pi}(g+1)(k_F a_p)^3}_{3} \underbrace{+ E_4(k_F)}_{4} + \mathcal{O}(k_F^5 \ln k_F)\Big]$$

I1–I6 (pp-hh ladders)
Kaiser, *Resummation of Fermionic In-Medium Ladders to All Orders*, NPA **860**

Regular diagrams
Baker, *Singularity Structure of the Perturbation Series for the Ground-State Energy of a Many-Fermion System*, RMP **43**

see also Baker, PRC **60**, 054311

diagrams with $*$ ($**$) have UV power (logarithmic) divergences

diagram	g factor	value
I1*	1	+0.0383115(0)
I2*+I3+I4*+I5*	1	+0.0148549(0)
I6	1	−0.0006851(0)
IA1	$g(g-3)+4$	−0.003623(1)
IA2	$g(g-3)+4$	−0.001672(1)
IA3	$g(g-3)+4$	−0.003343(1)
II1*+II2*	$g-3$	+0.058359(1)
II3+II4	$g-3$	−0.003358(1)
II5**	$g-3$	+0.0645(1)
II6**,*	$g-3$	−0.0265(2)
II7+II12	$g-3$	+0.003923(1)
II8+II11	$g-3$	+0.007667(1)
II9	$g-3$	−0.000981(1)
II10	$g-3$	−0.000347(1)
IIA1**	$3g-5$	+0.0647(1)
IIA2+IIA4	$3g-5$	+0.004122(1)
IIA3	$3g-5$	−0.000461(1)
IIA5	$3g-5$	+0.003542(1)
IIA6	$3g-5$	+0.003331(1)
III1***,**,*+III7+III8***,*	$g-1$	−0.0513(2)
III2***+III9+III10***	$g-1$	+0.001650(1)
$(\text{II5}+\text{IIA1})_{g=2}$	1	+0.00018(1)
$(\text{II6}+\text{III1}+\text{III7}+\text{III8})^*_{g=2}$	1	−0.0248(1)
$\sum_{\text{diagrams},g=2}$	1	−0.0425(1)

IR

Two-particle reducible diagrams

Wellenhofer, CD, and Schwenk,
PRC **104**, 014003 and PLB **802**, 135247

OHIO UNIVERSITY

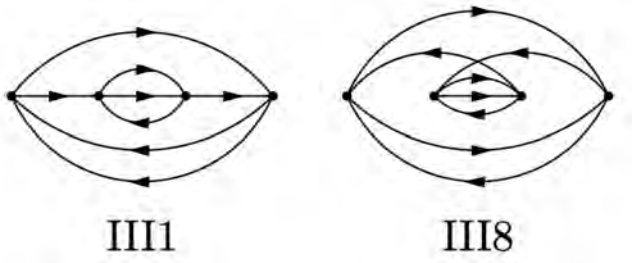

energy-denominator divergences

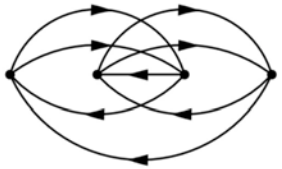

$$\frac{E_{4,\mathrm{III}(1+7+8)}}{\ln(\Lambda/k_\mathrm{F})} \xrightarrow{\Lambda\to\infty} \zeta(g-1)\frac{\sqrt{3}}{3^3 2^7 \pi^9}$$

Still diverges logarithmically

see also: Baker, Rev. Mod. Phys. **43**, 479 (Sec. III.C)
Feldman, Salmhofer, Trubowitz, J. Stat. Phys. **84**, 1209 (Sec. I)

$$E_{4,\mathrm{III}(1+7+8)} = -\zeta(g-1)\sum_{\substack{\mathbf{i,j,k}\\ \mathbf{a,c}}} n_{ijk}\bar{n}_{abc}\frac{\theta_{\mathbf{ab}}}{\mathcal{D}^2_{ab,ij}} \times\left(\bar{n}_d\frac{\theta_{\mathbf{ka}}\theta_{\mathbf{cd}}}{\mathcal{D}_{bcd,ijk}} - \bar{n}_{d'}\frac{\theta_{\mathbf{cd'}}}{\mathcal{D}_{cd',ik}}\right)\Bigg|_{\substack{\mathbf{b=i+j-a}\\ \mathbf{d=k+a-c}\\ \mathbf{d'=i+k-c}}},$$

$$\theta_{\mathbf{ab}} \equiv \theta(\Lambda/k_\mathrm{F} - |\mathbf{a}-\mathbf{b}|/2)$$
$$\mathcal{D}_{ab,ij} \equiv (a^2+b^2-i^2-j^2)/(2M)$$

cancels at the singularity:

$$\mathcal{D}_{ab,ij} = 0$$

energy-denominator divergences

- arise due to repeated energy denominators
- generic feature of zero-temperature MBPT
- are removed adding to their companions III(1+8) [also III(2+10)]

Suggests: evaluate diagrams in groups, *not* individually

- group diagrams according to their particle-hole content
- regularize energy denominators and probe sensitivity
- **improves overall numerical uncertainty & speed-up gains**

Ground-state energy: third order

Wellenhofer, CD, and Schwenk,
PRC **104**, 014003 and PLB **802**, 135247

OHIO UNIVERSITY

due to Pauli-blocking: expansion is analytic in (k_F a_s) for g = 2

3

$$E(k_\mathrm{F}) = E_0 \left(1 + \sum_{\nu=1}^{N} X_\nu \, (k_\mathrm{F} a_s)^\nu\right)$$

uncertainty estimate at order *N*

$$X_{N+1} = \pm \max[X_{\nu \le N}]$$

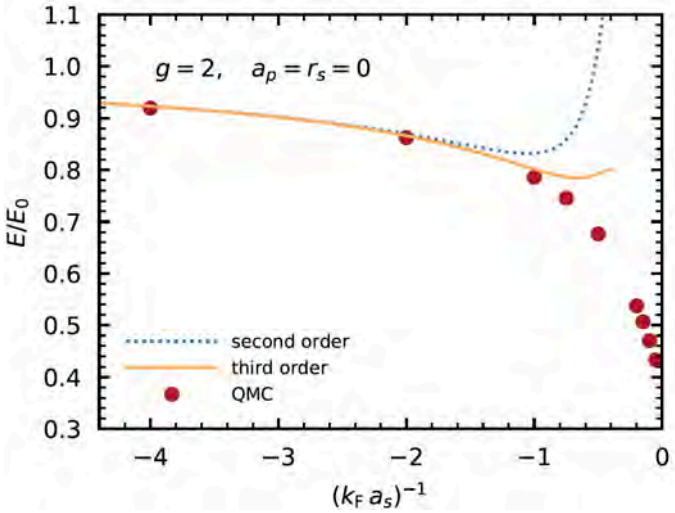

QMC: Gandolfi *et al.*, ARNPS **65**, 303

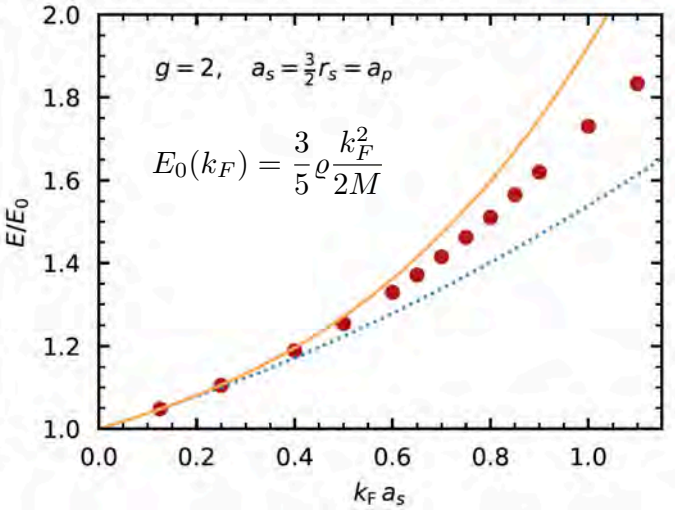

QMC: Pilati *et al.*, PRL **105**, 030405

Ground-state energy: fourth order

Wellenhofer, CD, and Schwenk,
PRC **104**, 014003 and PLB **802**, 135247

OHIO UNIVERSITY

due to Pauli-blocking: expansion is analytic in (k_F a_s) for g = 2

4

$$E(k_{\rm F}) = E_0 \left(1 + \sum_{\nu=1}^{N} X_\nu \, (k_{\rm F} a_s)^\nu \right)$$

uncertainty estimate at order *N*

$$X_{N+1} = \pm \max[X_{\nu \le N}]$$

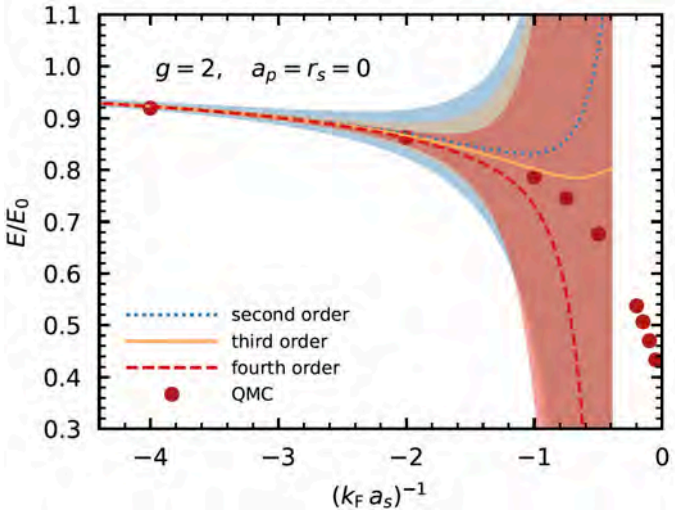

QMC: Gandolfi *et al.*, ARNPS **65**, 303

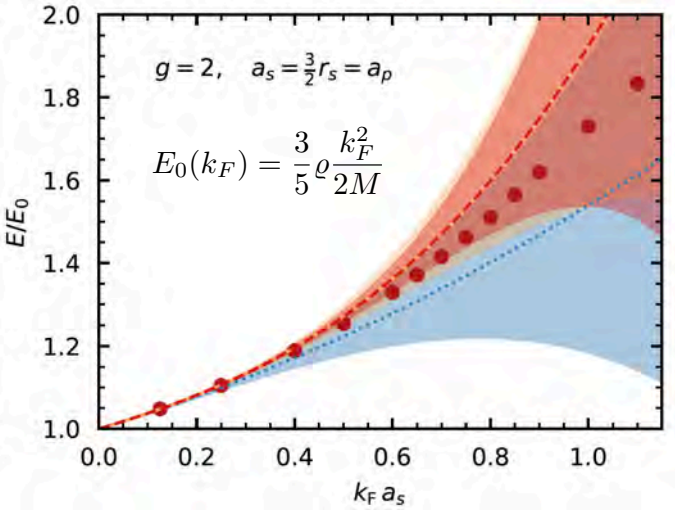

QMC: Pilati *et al.*, PRL **105**, 030405

Ground-state energy: fourth order

Wellenhofer, CD, and Schwenk,
PRC **104**, 014003 and PLB **802**, 135247

OHIO UNIVERSITY

4

due to Pauli-blocking: expansion is analytic in ($k_F\, a_s$) for g = 2

Bertsch parameter $\xi_n = 0.33\ldots0.54$

is consistent with cold atomic gases: $\xi_n = 0.45$

Ku *et al.*, Science **335**, 563

Padé resummation

$$[n,\, m] = \frac{\sum_{j=0}^{m} p_j x^j}{1 + \sum_{k=1}^{n} q_k x^k}$$

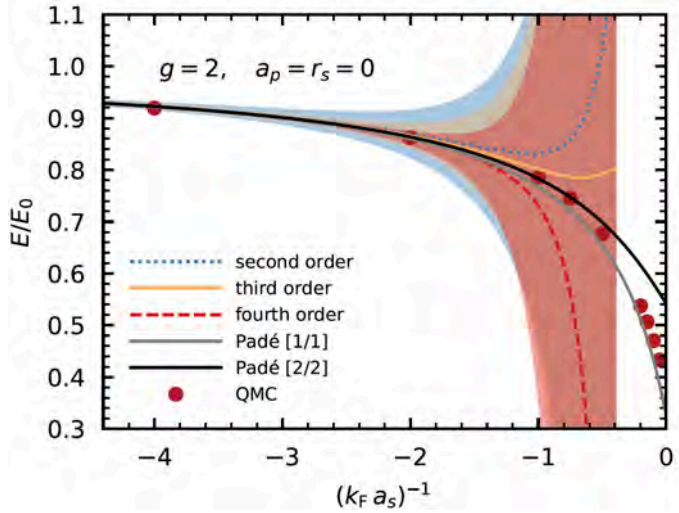

QMC: Gandolfi *et al.*, ARNPS **65**, 303

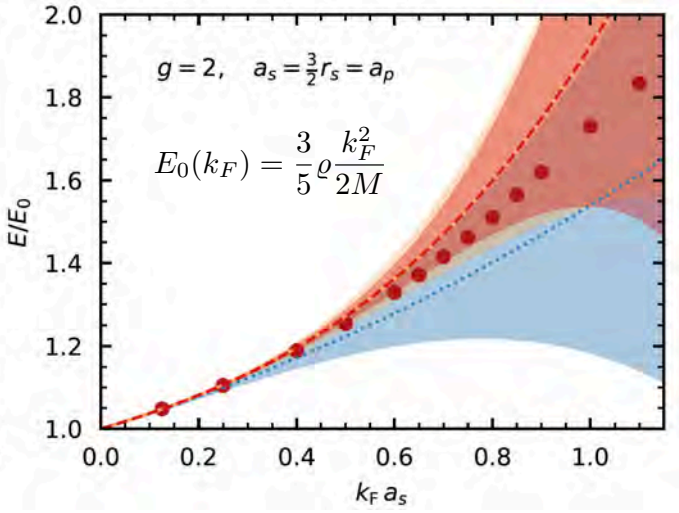

QMC: Pilati *et al.*, PRL **105**, 030405

More details? Recent review article

OHIO UNIVERSITY

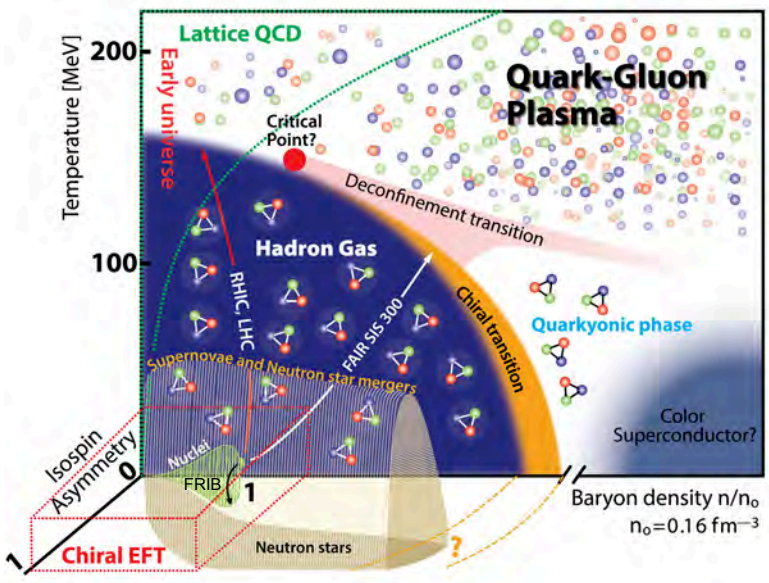

Keywords:

Chiral EFT | neutron stars | MBPT
nuclear matter at zero and finite temperature
Bayesian uncertainty quantification
recent neutron star observations

Chiral Effective Field Theory and the High-Density Nuclear Equation of State

Annual Review of Nuclear and Particle Science
Vol. 71:403-432 (Volume publication date September 2021)
First published as a Review in Advance on July 6, 2021
https://doi.org/10.1146/annurev-nucl-102419-041903

C. Drischler,[1,2,3] J.W. Holt,[4] and C. Wellenhofer[5,6]

[1]Department of Physics, University of California, Berkeley, California 94720, USA
[2]Nuclear Science Division, Lawrence Berkeley National Laboratory, Berkeley, California 94720, USA
[3]Facility for Rare Isotope Beams, Michigan State University, East Lansing, Michigan 48824, USA; email: drischler@frib.msu.edu
[4]Cyclotron Institute and Department of Physics and Astronomy, Texas A&M University, College Station, Texas 77843, USA
[5]Institut für Kernphysik, Technische Universität Darmstadt, 64289 Darmstadt, Germany
[6]ExtreMe Matter Institute EMMI, GSI Helmholtzzentrum für Schwerionenforschung GmbH, 64291 Darmstadt, Germany

see also in the same journal:
James Lattimer, Annu. Rev. Nucl. Part. Sci. **71**, 433

see also for finite nuclei:
Tichai, Roth, and Duguet, Front. Phys. **8**, 00164

Open Access

Take-away points

OHIO UNIVERSITY

multi-messenger
nuclear precision
FRIB
} era

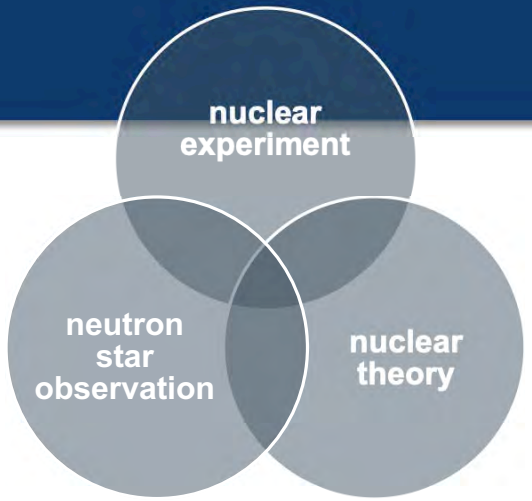

unique opportunity to obtain a **fundamental understanding** of strongly interacting matter, with great **potential for discoveries**

1. Upcoming observational (and experimental) campaigns will provide **stringent constraints** on the properties of neutron stars.
2. Chiral EFT enables **microscopic predictions** of nuclear matter (and nuclei) **with quantified uncertainties** to interpret these empirical constraints.
3. **Automated MBPT**: efficient EOS calculations across a wide range of densities, isospin asymmetries, and temperatures, as well as nuclear interactions.
4. Bayesian methods: powerful tools for quantifying & propagating **uncertainties** in EFT-based calculations (driven by fast & accurate emulators).

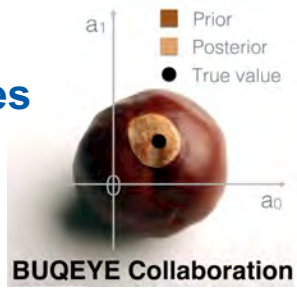

Many thanks to: R. Furnstahl A. Garcia P. Guiliani S. Han J. W. Holt J. Lattimer A. Lovell K. McElvain J. Melendez F. Nunes D. Phillips M. Prakash S. Reddy C. Wellenhofer X. Zhang T. Zhao

Interesting avenues (wish list?)

OHIO UNIVERSITY

Automated Diagram Generation (ADG):

- Automated identification of divergent diagram pairs
- residual 3N interactions ($n > 2$)
- different reference states (free, second order, …)
- finite temperature (anomalous, pole removal, $n > 3$)

How does Diagrammatic Monte Carlo handle these pairs?

MBPT convergence studies:

- Resummation methods (Padé, Borel, more advanced ML)
- Nonperturbative benchmarks
- (in-medium) Weinberg eigenvalue analysis (esp. *ph* channel)
- How does the SRG tame nonperturbative behaviour in different many-body channels?

How can we exploit the Petrov-Galerkin nature of coupled cluster equations?